



**Centrum voor Wiskunde en Informatica**  
Centre for Mathematics and Computer Science

---

F. van den Bosch, J.A.J. Metz, O. Diekmann

The velocity of spatial population expansion

Department of Applied Mathematics

Report AM-R8812

November

---

*Boelelaan 1077  
Centrum voor Wiskunde en Informatica  
Amsterdam*

The Centre for Mathematics and Computer Science is a research institute of the Stichting Mathematisch Centrum, which was founded on February 11, 1946, as a nonprofit institution aiming at the promotion of mathematics, computer science, and their applications. It is sponsored by the Dutch Government through the Netherlands Organization for the Advancement of Pure Research (Z.W.O.).

# The Velocity of Spatial Population Expansion

F. van den Bosch, J.A.J. Metz

*Institute of Theoretical Biology, State University of Leiden  
Groenhovenstraat 5, 2311 BT Leiden, The Netherlands*

O. Diekmann

*Centre for Mathematics and Computer Science  
P.O. Box 4079, 1009 AB Amsterdam, The Netherlands*

In this paper we consider the velocity with which an invading population spreads over space.

After a brief discussion about diffusion models, on the basis of which some terminology and intuition is developed, a much more general (linear) model, originally due to Diekmann and Thieme, is introduced. It will be seen that the asymptotic velocity of population expansion can be calculated if information is available on

- i. the net-reproduction,  $R_0$ ; i.e. the expected number of offspring produced by one individual throughout its life at infinitesimally small population density, and
- ii. the (normalized) reproduction-and-dispersal kernel,  $\beta(a, x - \xi)$ ; i.e. the density of newborns produced per unit of time at position  $x$  by an individual of age  $a$  born at  $\xi$ .

In a brief discussion we conjecture that the asymptotic velocity of population expansion of the linear model equals that of its non-linear modifications in a wide variety of cases. By means of numerical examples we study the effect of the net-reproduction and the shape of the reproduction-and-dispersal kernel on the velocity of population expansion. The fact that the reproduction-and-dispersal kernel is difficult to measure in full, leads us to derive approximation formulas in terms of easily measurable parameters. The relation between the velocity of population expansion as calculated from the general model and that from the, widely used, Fisher/Skellam model is discussed. As a final step we show that the model can quantitatively predict observed velocities of population expansion.

*1980 Mathematics Subject Classification:* 92A15.

*Key Words & Phrases:* integral equation, non-rotationally symmetric dispersal, approximation formulae, cumulant generating function, Fisher/Skellam model.

Report AM-R8812

Centre for Mathematics and Computer Science

P.O. Box 4079, 1009 AB Amsterdam, The Netherlands





0. Abstract
1. Introduction
2. Diffusion models
3. The linear model
  - 3.1. The integral equation for the birth rate
    - Individual behaviour
    - The birth rate equation
  - 3.2. The velocity of population expansion
    - Plane wave solutions
    - The asymptotic velocity of population expansion
    - Contours of equal birth rate
4. Non-linear models: how robust are the linear results?
5. Some numerical examples.
  - 5.1. Rotationally symmetric dispersal
    - Models for the dispersal density
    - Models for the reproduction kernel
    - Results
  - 5.2. Non-rotationally symmetric dispersal
    - The dispersal density
    - The reproduction kernel
    - Results
6. Various approximations
  - 6.1. Rotationally symmetric dispersal
    - Small  $R_0$
    - Concentrated reproduction kernels
  - 6.2. Non-rotationally symmetric dispersal
  - 6.3. Connections with the Fisher/Skellam velocity
    - Randomly moving individuals
    - Slow growing populations
7. Applications
  - 7.1. The Muskrat (*Ondatra zibethicus*)
  - 7.2. The collared dove (*Streptopelia decaocto*)
  - 7.3. Yellow rust (*Puccinia striiformis*)
  - 7.4. Downy mildew (*Peronospora farinosa*)
  - 7.5. Rabies (*Lyssavirus spp.*)
8. Discussion!
  - Appendix I. Derivation of the coefficients of (2.11) from the coefficients of (2.7)
  - Appendix II. Transformation of (3.5) into (3.6)

Appendix III. The relation between  $V(\rho)$  and  $C_0(\psi)$

Appendix IV. Derivation of formula (5.10)

Appendix V. A further connection with the Fisher/Skellam model

Appendix VI. The mean and variance of a stochastic block function

References

## 1. Introduction

Once upon a time a rich Czech prince went muskrat hunting in Alaska. He liked this so much that he took five muskrats back home and released them at his country-seat near Prague. These introduced individuals and their offspring started to spread, and nowadays considerable muskrat populations are established all over Europe.

This is just one of many well documented examples of biological invasions. A biological invasion can loosely be defined as a (on an evolutionary time scale) sudden extension of a populations range. Often such invasions are induced by man, as in the muskrat example. Others are the result of natural extensions of range. An epidemic of an infectious disease can be viewed as the expansion of a population of disease organisms and therefore also falls in the category of invasions.

Invading species often have an influence on the ecosystem and/or are economically important. This fact led the Scientific Committee on Problems of the Environment (SCOPE) to organize a programme on "The Ecology of Biological Invasions" (Anonymous, 1985). This programme addresses several questions concerning invasions, ranging from the invadability of ecosystems to the development of management systems to prevent unwanted invasions.

An invasion which starts at a certain place often does not have an immediate effect at an other, distant, place. The spatial component is, therefore, frequently of considerable importance. After the pioneering work of Fisher (1937), Skellam (1951), Kendall (1965) and Mollison (1972, 1977), Diekmann (1978, 1979) and Thieme (1977<sup>ab</sup>, 1979<sup>ab</sup>) developed and studied a rather general model for the spatial spread of populations. Using some of their main results we show in this paper how the velocity with which an invading population spreads over space depends on the population dynamical attributes of the individuals making up that population.

In order to develop some intuition, terminology and notation we start in section 2 with a discussion about diffusion models. Skellam (1951) was the first to investigate the velocity of population expansion, using such a diffusion model originally

derived by Fisher (1937) in a population genetic context. After a brief summary of the results of several authors on diffusion equation, we consider diffusion and convection in a linear model. (In section 6 we shall briefly return to the Fisher/Skellam model to discuss its role as an approximation to more complicated cases.) Next we turn to a more general model. After an explanation of the linear model we discuss the method to calculate the velocity of population expansion (section 3). In a brief discussion we conjecture that, in a wide variety of cases, the velocity of population expansion of the linear model and its non-linear refinements are equal (section 4). Some numerical examples show how the velocity of population expansion depends on the parameters of submodels describing the population dynamical attributes of the individuals (section 5). In practice, these attributes are difficult to measure in full. This leads us in section 6 to search for approximation formulas in terms of easily measurable parameters. Finally it will be shown that the model can indeed be used to predict, quantitatively, observed velocities of population expansion (section 7).

This paper is meant to bridge part of the gap between some abstract theorems about the velocity of population expansion in the mathematical and bio-mathematical literature and experimental biological practice. The paper is written for mathematically inclined biologists and mathematicians working on practical biological problems. Heuristic arguments and formal calculations abound in the paper. No proofs are given. In order not to hamper the progress of the story some calculations are postponed to appendices. Some of the results of heuristic arguments that need a more thorough mathematical investigation are formulated as conjectures.

## 2. Diffusion models

The simplest diffusion equation model for the spatial spread of a population in two dimensions reads

$$\frac{\partial n}{\partial t} = \frac{1}{2} s \left( \frac{\partial^2 n}{\partial x_1^2} + \frac{\partial^2 n}{\partial x_2^2} \right) + f(n)n \quad (2.1)$$

where  $n(t, x)$  is the population density at position  $x = (x_1, x_2)$  at time  $t$ ,  $s$  is the 'diffusion constant' indicating the rate of random movement and  $f(n)$  is the per capita 'population growth rate' as a function of local population density. For  $f(n)$  we assume that  $f'(n) \leq 0$  for all  $n \geq 0$ .

First consider the linear equation obtained by putting  $f(n) = f(0)$ , for all  $n$ . The solution of this equation for the initial condition

$$n(0, x) = \delta(x) \quad (2.2)$$

is given explicitly by

$$n(t, x) = \frac{1}{2\pi st} \exp\left(-\frac{|x|^2}{2st} + f(0)t\right). \quad (2.3)$$

It is easily seen that for any  $\varepsilon (> 0)$

$$n(t, x) \xrightarrow{t \rightarrow \infty} \begin{cases} 0 & \text{if } |x| > (C_0 + \varepsilon) t \\ \infty & \text{if } |x| < (C_0 - \varepsilon) t \end{cases} \quad (2.4)$$

where

$$C_0 = \sqrt{2 s f(0)}. \quad (2.5)$$

(2.4) states that if one travels in a straight line away from the origin with a velocity larger (smaller) than  $C_0$ , one will, in the long run, observe a population with density zero (infinity). In this sense  $C_0$  is the asymptotic velocity of population expansion. From (2.3) it is also seen that contours of equal population density behave like expanding circles. The radius of these circles increases as  $C_0 t$  for  $t \rightarrow \infty$ . Contours of equal rate of population change,  $\frac{\partial n}{\partial t}$ , behave in the same way.

The non-linear model (2.1) cannot be solved explicitly. In order to calculate the velocity of population expansion recourse is taken to the investigation of so-called travelling plane wave solutions of (2.1). Such a solution has the form

$$n(t, x) = \tilde{n}(x \cdot v - C t) \quad (2.6)$$

where  $C (\geq 0)$  is the velocity of the wave and  $v$  is a unit vector giving the direction of movement. Such a solution can be visualized as a function of  $x$ , which has, at a given time, a constant value on lines  $x \cdot v = \text{constant}$ . This function of  $x$  is shifted with constant velocity,  $C$ , in the direction  $v$  without any change in shape. Substitution of (2.6) in (2.1) yields an ordinary differential equation for  $\tilde{n}$ . From this equation it can be shown (e.g. Fisher, 1937; Aronson and Weinberger, 1975; Haderler and Rothe, 1975; Diekmann and Temme, 1976) that (2.1) has travelling plane wave solutions for every  $C \geq C_0$ , where  $C_0$  is defined by (2.5). The velocity  $C_0$  will therefore be called the minimal wave velocity. Note that, due to the rotational symmetry of the problem, the value of  $C_0$  does not depend on the direction  $v$ .

From the work of Aronson and Weinberger (1975,1978), it can be concluded that, at least for initial conditions with a bounded spatial support, (2.4) still holds if we replace the ' $\rho$ ' at the right hand side by  $\hat{n}$ , where  $\hat{n}$  is the solution of  $f(\hat{n}) = 0$ . (Various more subtle aspects of the convergence of solutions of (2.1) to travelling wave solutions have been studied in the one-dimensional case, e.g. Kolmogorov, Petrovsky and Piskounov (1937), and Bramson (1983).) Note that founder populations always have a bounded spatial support. So,  $C_0$  is again the asymptotic velocity of population expansion and the density dependence has not changed it.

A physical analogue makes the fact that the minimal wave velocity is also the asymptotic velocity intuitively clear. Imagine that we align a large number of fire-pots so that they can kindle each other. Furthermore, attach to each pot a piece of slowmatch that can set fire to that particular pot separately. We can now create (the illusion of) a travelling wave by (at  $t=0$ ) simultaneously setting fire to the pieces of slowmatch at distances from the firepot which increase linearly with the serial number of the pots. By changing the steepness of this linear relation we can create waves with different velocities. However, if we try to make the velocity too small the cross kindling takes over. Consequently the velocity produced by cross kindling necessarily corresponds to the lowest possible wave velocity. If we set fire to only a small number of slowmatches at

one end of the line of firepots (the analog of a founder population with bounded support) this will always produce a wave of burning firepots with the minimal velocity.

Sometimes the dispersion of individuals is not isotropic (rotationally symmetric), as is assumed in (2.1). Diffusion rates may be different in the various directions or there may be a systematic movement of individuals in a certain direction, for example due to a prevailing wind direction. In the rotationally symmetric (linear) case the circularity of contours of equal population density makes that the (minimal) velocity of a traveling plane wave solution is equal to the asymptotic velocity of population expansion along any straight line from the origin. In the non-rotationally symmetric case contours of equal population density are not circular and the two velocities differ (Figure I). As a simple example we consider the linear diffusion model:

$$\frac{\partial n}{\partial t} = - \sum_i m_i \frac{\partial n}{\partial x_i} + \frac{1}{2} \sum_{ij} s_{ij} \frac{\partial^2 n}{\partial x_i \partial x_j} + f(0)n ; \quad (2.7)$$

$i, j=1, 2$  and  $s_{12}=s_{21}$ .

With initial condition

$$n(0, x_1, x_2) = \delta(x),$$

the solution of (2.7) is

$$n(t, x_1, x_2) = \frac{\exp[f(0)t - \frac{1}{2t} (X-Mt)^T S^{-1} (X-Mt)]}{2 \pi t \sqrt{\det S}} \quad (2.8)$$

where  $X = (x_1, x_2)^T$ ,  $M = (m_1, m_2)^T$ ,  $S = (s_{ij})$  and  $\det S$  is the determinant of the matrix  $S$ . Contours of equal population density are for  $t \rightarrow \infty$  given by

$$(X-Mt)^T S^{-1} (X-Mt) = 2 f(0) t^2 . \quad (2.9)$$

These are expanding ellipses with their centre at  $Mt$ , and axes in the direction of the eigenvectors of  $S$ . The length of the axes is given by  $\lambda_i \sqrt{2f(0)} t$ , where the  $\lambda_i$  are the corresponding eigenvalues (figure 1). From this, the asymptotic velocity,  $V(\rho)$ , of population expansion along a straight line from the origin making an angle  $\rho$  with the  $x_1$ -axis is

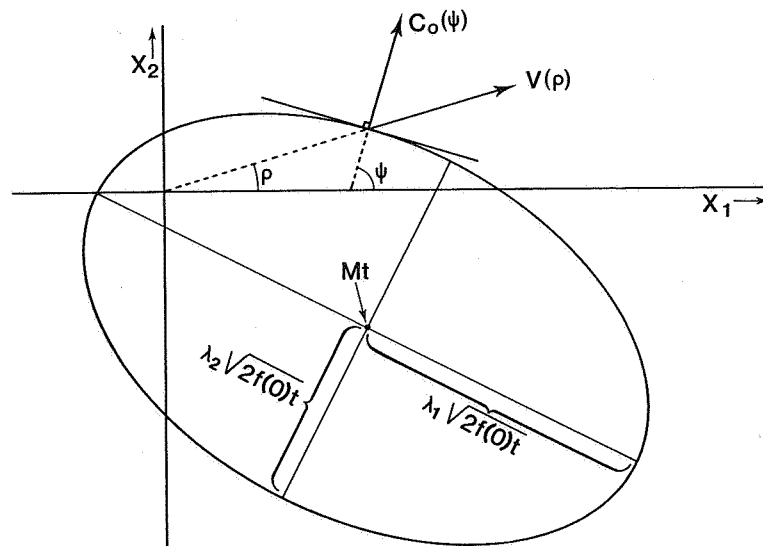


figure 1: Contours of equal population density for a (linear) diffusion model with convection (equation (2.7)). The contours are expanding ellipses, with centre and the, orientation and length of the axis as given in section 2. The figure also illustrates the difference between the velocity of a plane population,  $C_0(\psi)$ , and the velocity of population expansion on a straight line from the origin,  $V(\rho)$ .

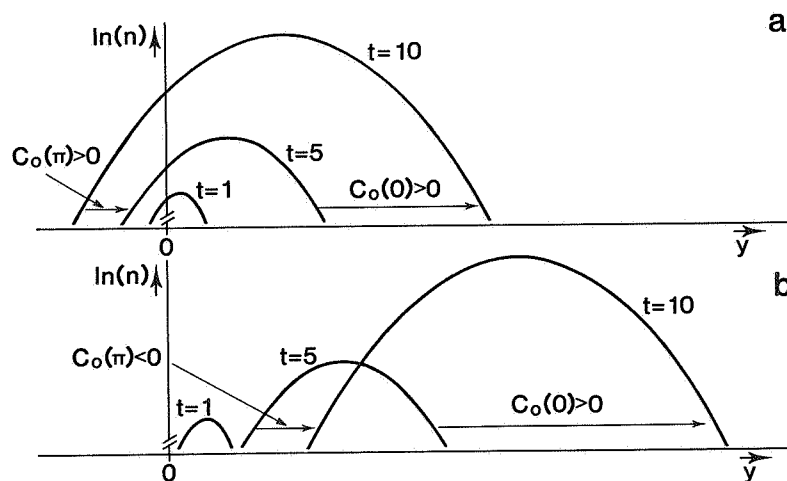


figure 2: The solution of a linear diffusion model with convection (equation (2.11)). Horizontal: distance  $y$ , vertical: number of individuals,  $n$  (log scale). In figure a the convection velocity,  $m$ , is small compared to the diffusion coefficient and the population growth rate. The velocities of population expansion in both the positive and the negative  $y$  direction are therefore positive. In figure b convection is much larger, resulting in a negative velocity in the negative  $y$  direction.



$$V(\rho) = \frac{-(s_{12}m_2 - s_{22}m_1) \cos \rho + (s_{12}m_1 - s_{11}m_2) \sin \rho \pm \sqrt{Q(\rho)}}{s_{22} \cos^2 \rho - 2s_{12} \cos \rho \sin \rho + s_{11} \sin^2 \rho} \quad (2.10)$$

where

$$Q(\rho) = [(s_{12}m_2 - s_{22}m_1) \cos \rho + (s_{12}m_1 - s_{11}m_2) \sin \rho]^2 - (s_{22} \cos^2 \rho - 2s_{12} \cos \rho \sin \rho + s_{11} \sin^2 \rho) \cdot [(s_{22}m_1^2 - 2s_{12}m_1m_2 + s_{11}m_2^2 + 2(s_{12}^2 - s_{11}s_{22}) f(0)].$$

The collection of vectors  $V(\rho)$  gives the shape of the contour of equal population density and is presented as the ellipse in figure 1 with  $t=1$ .

On the other hand, the asymptotic velocity of a plane wave front moving in the direction  $x_1 = (y \cos \psi)$ ,  $x_2 = (y \sin \psi)$  can be calculated from the following one dimensional version of (2.7) (see appendix I):

$$\frac{\partial n}{\partial t} = -m \frac{\partial n}{\partial y} + \frac{1}{2} s \frac{\partial^2 n}{\partial y^2} + f(0) n \quad (2.11)$$

with coefficients

$$m = (\cos \psi, \sin \psi) M ; s = (\cos \psi, \sin \psi) S \begin{pmatrix} \cos \psi \\ \sin \psi \end{pmatrix}. \quad (2.12)$$

The solution of (2.11) corresponding to a Dirac mass initial condition is given by (2.3) if we substitute  $|y-mt|$  for  $|x|$ . This gives

$$C_0(\psi) = (m_1 \cos \psi + m_2 \sin \psi) \pm \sqrt{2 f(0) \tilde{P}(\psi)} \quad (2.13)$$

where

$$\tilde{P}(\psi) = s_{11} \cos^2 \psi + 2 s_{12} \cos \psi \sin \psi + s_{22} \sin^2 \psi.$$

The solution of (2.11) can be visualized as a (moving) function of  $y$  which has the shape of a Gaussian density the area of which increases exponentially and which shifts with velocity  $m$  in the positive direction (figure 2). It is obvious that when  $m$  is large enough, compared to  $s$  and  $f(0)$ , the population does not build up

in the negative direction. The asymptotic velocity in that direction is then negative. For instance, consider equation (2.13); when  $m_1 > \sqrt{2f(0) \tilde{P}(\psi)}$ , there is a (large) positive  $C_0(\psi)$  if one looks in the  $\psi=0$  direction and a (small) negative  $C_0(\psi)$  if one looks in the opposite direction ( $\psi=\pi$ ). This is illustrated in figure 2<sup>b</sup>. Similarly, when  $M$  is large enough, the ellipse (2.9) does not enclose the origin.

Diffusion equations, such as (2.1), are often applied in studies on the spatial spread of populations (Okubo, 1986; Williamson and Brown, 1986; Lubina and Levin, 1988; Källén, Arcuri and Murray, 1985; Caughley, 1970; Watt, 1968; Noble, 1974). Although much valuable insight has been gained from these studies, there is an inherent draw-back to the use of the diffusion equation formulation. These equations make very specific assumptions about the processes at the individual level, to wit: (i) every individual moves at random throughout its life, (ii) the reproduction- and death-rate of the individuals only depend on their local environment (be it constant,  $f(0)$ , or dependent on population density,  $f(n)$ ). The life history of species generally is more complicated. For example, reproduction- and death-rates may depend on age, or an individual may settle down permanently on a breeding ground at the end of its juvenile period. It is interesting to know how the velocity of population expansion is related to the life history of the individuals comprising the population.

In practical applications it are quantities like the probability to survive to a certain age and the settlement pattern of juveniles that can be derived experimentally. The question then is how we can calculate the velocity of population expansion from such experimentally observed quantities.

In the following section we shall present a modelling framework which allows us to answer these questions.

### 3. The linear model

#### 3.1. The integral equation for the birth rate.

In the linear model we assume the environment to be constant. This entails a fixed relation between age and the average population dynamical behaviour (rate of giving birth, probability of dying, etc.) of an individual (provided 'individuals are born equal'). Therefore we can write down an age structured model (compare Metz & Diekmann, 1986, chapter IV). Before deriving the birth rate equation we first discuss in some detail the appropriate description of the average behaviour of an individual.

Although the model is of a general nature we will use a terminology proper to animal species in the main text. In some examples we use a different, but compatible, terminology proper to the species under consideration. For species with two sexes we consider females only.

Individual behaviour: A model intended to describe the spatial spread of a wide variety of species should incorporate as few assumptions as possible about reproduction and dispersal at the individual level. We define the function  $\tilde{B}(a, x, \xi)$  to be the density of newborns produced per unit of time at position  $x$  by an individual of age  $a$  born at  $\xi$ , ( $x, \xi \in \mathbb{R}^2$ ).  $\tilde{B}$  will be called the reproduction-and-dispersal kernel.

Example 1. For mammals and birds  $\tilde{B}$  incorporates both the demographic and the dispersal characteristics of an individual. The demographic characteristics are the two basic life-table statistics; (i) the probability that an individual is still alive at age  $a$ ,  $L(a)$ , usually called the age specific survivorship and (ii) the rate of offspring production of an individual at age  $a$ ,  $m(a)$ . The dispersal characteristic is the conditional dispersal density,  $D^*(a, x, \xi | \text{alive})$ , which is defined as the probability that an individual born at  $\xi$  is living at  $x$  when it has age  $a$ , given that it is still alive. The reproduction-and-dispersal kernel is given by

$$\tilde{B}(a, x, \xi) = L(a) m(a) D^*(a, x, \xi | \text{alive}).$$

Example 2. For infectious diseases the definition of 'individual' requires some care. For some diseases one pathogen individual is equivalent to one individual in our model. Such is, for instance, the case in a fungal disease causing lesions on a plant leaf. In other cases a complete population of pathogen individuals localized in one host is equivalent to one 'individual' in our model. For instance, one fox is one 'individual' if we consider rabies, while a rabid fox contains millions of rabies viruses. For any particular disease, 'individual' has to be chosen such that we can assume that, once infected, the course of the 'individual's' infectivity is an autonomous process. Now define the infectivity  $I(a)$ , to be the number of new infections caused per unit of time by an individual which has been infected time  $a$  ago.  $I(a)$  includes the probability that the individual is still alive.

The precise biological interpretation of the dispersal density,  $D^*(a, x, \xi | \text{alive})$  depends on the transfer mechanism of the pathogen species. When the disease is transmitted through physical contacts between animals,  $D^*$  is the probability that a host individual having its centre of activity at  $\xi$  infects, at age of illness  $a$ , a host having its centre of activity at  $x$ . When the infection is transmitted through air-borne spores, as in many fungi on plants,  $D$  is the probability that a spore released at  $\xi$ , infects a plant at  $x$ .

By definition,  $B(a, x, \xi) = I(a) D^*(a, x, \xi | \text{alive})$ .

Throughout this paper we assume  $\tilde{B}$  to be translationally invariant (homogeneity of the habitat). So,

$$\tilde{B}(a, x, \xi) = B(a, x - \xi).$$

When  $B$  is rotationally symmetric it is a function of the distance  $|x - \xi|$  only.

The function  $B$  can be normalized by defining

$$\beta(a, x - \xi) = R_0^{-1} B(a, x - \xi) \quad (3.1^a)$$

where

$$R_0 = \int_0^{\infty} \int_{\mathbb{R}^2} B(a, x) dx da \quad (3.1^b)$$

is the expected total number of offspring produced by one individual throughout its whole life. This quantity is known as the net-reproduction. We assume that  $B$  is such that this integral exists and is finite. It is obvious that a necessary and sufficient condition for a population to grow if it is infinitesimally small is  $R_0 > 1$ . Throughout this paper we restrict our attention to this situation. Note that  $\beta$  can be interpreted as a probability density.  $\beta$  will be called the normalized reproduction-and-dispersal kernel.

Note: It should be pointed out that, in the ecological literature ' $R_0$ ' and the term 'net-reproduction' are sometimes used also for the density dependent case. Density dependence can be considered as the result of a feedback through the environment of the individuals (Metz and Diekmann, 1986). Let  $E(t,x)$  denote the condition of the environment at time  $t$  at position  $x$  as experienced by the individuals. If  $E(t,x) = \tilde{E}$  we can define  $R(\tilde{E})$  to be the total expected lifetime offspring number under environmental condition  $\tilde{E}$ . If  $\tilde{E}_0$  denotes the condition of the virgin environment, assumed to be constant, then  $R_0 = R(\tilde{E}_0)$ . Throughout this paper we will use  $R_0$  in this sense.

The marginal density

$$\beta^0(a) = \int_{\mathbb{R}} \beta(a,x) dx, \quad (3.2)$$

is the probability density of a random variable called 'the age-at-child-bearing'. A biological interpretation of  $\beta^0$  can be found in Metz and Diekmann (1986, page 153).  $\beta^0(a)$  will be called the reproduction kernel. The marginal density

$$D(x) = \int_0^{\infty} \beta(a,x) da, \quad (3.3)$$

is called the dispersal density. It is the probability density of the place of birth of an average offspring from an individual born at  $\bar{0}$ .

We shall frequently assume that reproduction and dispersal are statistically independent, i.e.:

$$\beta(a,x) = \beta^0(a) \cdot D(x). \quad (3.4)$$

Note the difference between statistical independence and the mechanistic independence incorporated in, for example, the

diffusion models. Although dispersal rates in such models are independent of age the resulting dispersal density is a function of age and (3.4) does not apply.

Example 1, continued: When individuals of a species first disperse and then settle down permanently on their breeding-ground at the end of the juvenile period, (3.4) applies.

Example 2, continued: When the relative frequency with which places within its homerange are visited by an individual does not change during the course of its illness, such as seems to be more or less the case for rabid foxes, (3.4) applies. When the dispersal of fungal spores takes place at a much shorter time scale than the time scale of spore production we can again use (3.4).

The birth rate equation: Denote by  $b(t,x)$  the number of births per unit of area and per unit of time at position  $x$  at time  $t$ . This quantity equals the sum of all current births at  $x$  from parents of all possible ages born at all possible places. The current births due to parents of age  $a$  born at  $\xi$  is equal to the number (actually the density) of parents born time  $a$  ago at  $\xi$ ,  $b(t-a,\xi)$ , times their per capita rate of offspring production at  $x$ ,  $R_0 \beta(a,x-\xi)$ . The population equation therefore takes the form:

$$b(t,x) = R_0 \int_0^{\infty} \int_{\mathbb{R}^2} b(t-a,\xi) \beta(a,x-\xi) d\xi da . \quad (3.5)$$

Note that this equation is a spatial variant of the renewal equation, originally due to Lotka, which is used in demography.

Remark I: Actually the time integral only extends backwards till the time the population was founded and we also have to describe the influence of the founder population. However, in this paper we are only interested in the asymptotic behaviour of the model and we can therefore restrict our attention to (3.5).

Remark II: The total number of individuals at position  $x$  at time  $t$ ,  $n(t,x)$ , can be calculated from

$$n(t,x) = \int_0^{\infty} \int_{\mathbb{R}^2} b(t-a,\xi) \mathcal{L}(a,x-\xi) d\xi da \quad (3.6)$$

where  $\mathcal{L}(a,x-\xi)$  is the probability that an individual of age  $a$  born at  $\xi$  is alive and living at  $x$ . Since no individual lives

forever it is reasonable to assume that  $\mathcal{L}$  is such that this integral exists and is finite.

### 3.2. The velocity of population expansion.

Plane wave solutions: Travelling plane wave solutions of (3.5) have the form

$$b(t, x) = \tilde{b}(Ct - x \cdot v)$$

where  $v = (\cos \psi, \sin \psi)^T$  for some  $\psi \in [0, 2\pi)$ . Substitution of the trial solution

$$\tilde{b}(Ct - x \cdot v) = \zeta \exp(\lambda(Ct - x \cdot v)), \quad (3.7)$$

leads to the characteristic equation

$$L(C, \lambda) = 1 \quad (3.8)$$

where

$$L(C, \lambda) = R_0 \int_0^\infty \int_{\mathbb{R}^2} e^{-\lambda(Ca - \xi \cdot v)} \beta(a, \xi) d\xi da.$$

Applying the transformation ( $\xi'_1 = \xi_1 \cos \psi + \xi_2 \sin \psi$ ;  $\xi'_2 = -\xi_1 \sin \psi + \xi_2 \cos \psi$ ) and immediately dropping the primes again yields (see appendix II)

$$L(C, \lambda) = R_0 \int_0^\infty \int_{-\infty}^\infty e^{-\lambda(Ca - \xi)} \tilde{\beta}(a, \xi_1) d\xi_1 da \quad (3.9^a)$$

where

$$\tilde{\beta}(a, \xi_1) = \int_{-\infty}^\infty \beta(a; \xi_1 \cos \psi - \xi_2 \sin \psi, \xi_1 \sin \psi + \xi_2 \cos \psi) d\xi_2. \quad (3.9^b)$$

Note that  $\tilde{\beta}$  is the marginal-distribution of  $\beta$  over the line  $x \cdot v = 0$ . When  $\lambda$  and  $C$  are chosen such that (3.8) has a solution, there exists a travelling wave solution of the form (3.7) for the population equation (3.5). First note that a solution of (3.8) for which  $\lambda < 0$ ,  $(\tilde{\lambda}, \tilde{C})$  say, corresponds to a solution with positive  $\lambda$ ;  $(-\tilde{\lambda}, -\tilde{C})$  if one substitutes  $\xi_1 = -\xi_1'$  in the kernel  $\tilde{\beta}$  in (3.9). This can be visualized as follows: Consider an observer

looking in a certain direction and seeing a travelling wave  $(\tilde{\lambda}, \tilde{C})$ . Next the observer turns around  $\pi$  rad. and looks in the opposite direction. He will now see the same travelling wave but it now has  $(-\tilde{\lambda}, -\tilde{C})$  as its parameters. We conclude that, without loss of generality, we can restrict our attention to  $\lambda \geq 0$ .

For rotationally symmetric  $\beta$  the existence of solutions of (3.8) was studied by Diekmann (1978). He noted that: (i)  $L$  is defined in a (right hand) neighbourhood of  $\lambda = 0$ ; (ii) for fixed  $C$ ,  $L$  is a convex function of  $\lambda$ , (iii) for every  $\lambda > 0$ ,  $L$  is a decreasing function of  $C$  and (iv)  $\left. \frac{\partial L}{\partial \lambda} \right|_{\lambda=0} < (=) 0$  for  $C > (=) 0$ .

In the non-rotationally symmetric case (iv) becomes

$$\left. \frac{\partial L}{\partial \lambda} \right|_{\lambda=0} = R_0 (\bar{\xi}_1 - C \bar{a}) \quad (3.10)$$

where

$$\bar{\xi}_1 = \int_0^{\infty} \int_{-\infty}^{\infty} \xi_1 \beta(a, \xi_1) d\xi_1 da$$

and

$$\bar{a} = \int_0^{\infty} \int_{-\infty}^{\infty} a \beta(a, \xi_1) d\xi_1 da .$$

Furthermore Diekmann restricted attention to  $C > 0$ , which is reasonable in the rotationally symmetric case. In the non-rotationally symmetric case there can be solutions with  $C \leq 0$ , as we saw in the diffusion equation model in chapter 2. Such solutions are possible when  $\tilde{\beta}$  is very skewed. In this situation the number of offspring that an individual produces in a certain direction is so small that the population does not build up in that direction. The result is a retracting population wave. (In section 5 an example is given where we find negative velocities). In addition to (iii), we note that  $L$  is defined for  $C \in (c_1, c_2)$ , where  $c_1 \leq 0$ ,  $c_2 > c_1$  and  $c_1, c_2 \in \mathbb{R}$ . Furthermore, if  $C \downarrow c_1$ ,  $L \rightarrow \infty$ , and (iii) holds for every  $C \in (c_1, c_2)$ .

Now, under our assumption  $R_0 > 1$  and following the same reasoning as in Diekmann (1978) it can be concluded that there is a  $C_0 \in \mathbb{R}$  such that there exist travelling wave solutions of (3.5) for every  $C \geq C_0$ . This  $C_0$  can be calculated from



$$\begin{aligned}
 L(C_0, \lambda_0) &= 1 \\
 \frac{\partial L}{\partial \lambda} (C_0, \lambda_0) &= 0 .
 \end{aligned}
 \tag{3.11}$$

The asymptotic velocity of population expansion: For rotationally symmetric  $\beta$ . the n-dimensional version of equation (3.5) is a special case of the model studied by Diekmann (1978, 1979) and Thieme (1977, 1979). They proved that, at least if one makes the biologically reasonable assumption that the founder population has bounded support,  $C_0$  is the asymptotic velocity of population expansion in the sense of equation (2.4). In an n-dimensional discrete time model originally derived in a population genetic context, Weinberger (1978, 1982) showed that the minimal wave velocity of plane fronts suffices to describe the asymptotic velocity of spread also in the non-rotationally symmetric case. (For related work of Lui we refer to Creegan and Lui (1984) and the references given there.) Although a proof for the continuous version of the non-rotationally symmetric case is still lacking, we are convinced that one can safely assume that the minimal wave velocity of plane fronts,  $C_0$ , determines (in a manner described below) the asymptotic velocity of population expansion for the population model (3.5).

Contours of equal birth rate. As discussed in section 2 there is a difference between the minimal velocity,  $C_0(\psi)$ , of a plane wave travelling in a direction which makes an angle  $\psi$  with the  $x_1$ -axis, and the asymptotic velocity,  $V(\rho)$  of population expansion along a straight line from the origin making an angle  $\rho$  with the  $x_1$ -axis (figure 1). We may now pose the following problem: given  $C_0(\psi)$ , how can we calculate  $V(\rho)$ ? In appendix III we derive that, under the biologically reasonable assumption that  $V$  is a smooth function of  $\rho$ ,  $V$  and  $C_0$  are related by

$$\begin{aligned}
 V(\rho) \cos (\psi-\rho) &= C_0(\psi) \\
 -V(\rho) \sin (\psi-\rho) &= C_0'(\psi) .
 \end{aligned}
 \tag{3.12}$$

In concrete calculations we may vary  $\psi$  from 0 to  $2\pi$  and solve (3.12) for  $V$  and  $\rho$ . The collection of pairs  $(\rho, V)$  so obtained yields the 'graph' of  $V$ . The 'graph' of  $V$  is directly related to the contours of equal birth rate. Looking at the population from

high up in the air we will see that for sufficiently large  $t$  these contours are approximately given by

$$\{(V(\rho) \cos(\rho)t, V(\rho) \sin(\rho)t) \mid \rho \in [0, 2\pi)\}.$$

(In appendix III we indicate in which sense the phrase "are approximately given" should be interpreted.)

Remark: In his paper on a discrete time model for the spatial spread of genes, Weinberger (1983) also considers the relation between  $C_0(\psi)$  and  $V(\rho)$ . In appendix III we show how Weinbergers' results are related to (3.12).

#### 4. Non-linear models : how robust are the linear results?

So far we only considered density independent population growth. Of course, populations will not grow beyond every bound. At the higher densities the population will, through its influence on its environment which in its turn influences the birth-and-dispersal kernel, change its own dynamical properties. Is the velocity of population expansion in the non-linear case equal to the one in the linear case?

Diekmann (1978, 1979) and Thieme (1977<sup>ab</sup>, 1979<sup>ab</sup>) investigated, for rotationally symmetric dispersal, a special type of non-linearity. In his discrete time model Weinberger (1982) investigated a similar type of non-linearity, and he included non-rotationally symmetric dispersal. Both Diekmann & Thieme and Weinberger showed that the minimal velocity of population expansion of the corresponding linear model is still the asymptotic velocity of population expansion of the full non-linear variant. The particular types of density dependence considered by these authors have clear biological relevance (at least for the spatial spread of infectious diseases, Diekmann and Thieme, and for the spatial spread of genes, Weinberger) and the results give much insight. One would, however, like to have results on non-linear models where the density dependent feedback is of a more general nature.

When a wide variety of density dependent feedbacks is allowed, the possibility of population oscillations or the eventual extinction of the species in the case of non-renewable resources

has to be taken into account. This can cause problems with our definition of asymptotic velocity from section 2, so a slight readjustment will be necessary. A possible way to define the asymptotic velocity,  $V(\rho)$ , is by requiring it to satisfy

i) For any  $\varepsilon > 0$  and every  $\rho \in [0, 2\pi)$

$$\limsup_{t \rightarrow \infty} \sup_{\tau > t} b(t, V(\rho) \begin{pmatrix} \cos \rho \\ \sin \rho \end{pmatrix} (1+\varepsilon)\tau) = 0. \quad (4.1^a)$$

ii) There is a  $\eta > 0$  such that for any  $\varepsilon > 0$  and every  $\rho \in [0, 2\pi)$

$$\liminf_{t \rightarrow \infty} \sup_{\tau > t} b(t, V(\rho) \begin{pmatrix} \cos \rho \\ \sin \rho \end{pmatrix} (1-\varepsilon)\tau) > \eta. \quad (4.1^b)$$

In words i) again means that if one travels in a straight line away from the origin at a velocity larger than  $V$  one will 'outrun' the birth wave. For the interpretation of ii) consider the expanding closed contour of places where the birth rate reaches a certain small quantity for the first time. Now ii) states that if one travels with a velocity smaller than  $V$  one will in the long run end up inside this expanding contour.

According to the physiologically structured population creed, any density dependence should be considered as being the result of a feedback through the environment of the individual (Metz and Diekmann, 1986).

Example I: A size-structured herbivore-plant system.

Assume that a particular herbivore individual can be characterized by its weight,  $w$ , and assume that it moves at random through space. Let  $E(t, x)$  denote the plant density at time  $t$  at position  $x$  (the choice of the letter  $E$  indicates that we think of this plant density as the relevant indicator of the environmental condition) and let  $n(t, x, w)$  denote the weight distribution of the herbivore population at time  $t$  at position  $x$ . The evolution of this distribution is governed by

$$\begin{aligned} \frac{\partial n(t, x, w)}{\partial t} = & - \frac{\partial g(w, E(t, x)) n(t, x, w)}{\partial w} + s(w, E(t, x)) \frac{\partial^2 n}{\partial x^2} - \\ & - \mu(w, E(t, x)) n(t, x, w) \end{aligned} \quad (4.2^a)$$

where  $g$  is the individual growth rate, which is assumed to be a non-decreasing function of  $E$ , and  $\mu$  is the per capita death rate, assumed to be non-increasing with  $E$ . Moreover,  $g$ ,  $s$  and  $\mu$  are assumed to be sufficiently smooth. The boundary condition has the form

$$g(w_0, E(t, x))n(t, x, w_0) = b(t, x) \quad (4.2^b)$$

where  $w_0$  is the weight at birth and

$$b(t, x) = \int m(w, E(t, x))n(t, x, w)dw \quad (4.2^c)$$

where  $m$  is the expected number of young produced per unit of time by an herbivore individual;  $m$  is assumed to be sufficiently smooth and to be decreasing in  $E$  and non-decreasing in  $w$ . This completes the specification of the herbivore population model.

First assume  $E(t, x)$  to be given. Consider the probability,  $P(t, x, w | t_0, x_0, E)$ , that an individual born at  $t_0$  at position  $x_0$  is at time  $t$ , at position  $x$  and has size  $w$ . This probability satisfies equation (4.2<sup>a</sup>) with

$$P(t_0, x_0, w | t_0, x_0, E) = \delta(x - x_0) \delta(w - w_0),$$

and boundary condition

$$P(t, x, w_0 | t_0, x_0, E) = 0.$$

We shall moreover set  $P = 0$  for  $t < t_0$ . If we know  $P$  we can calculate the population birth rate  $b$  at  $x$  from

$$b(t, x) = \iint \tilde{B}(a, x | t-a, \xi, E) b(t-a, \xi) da d\xi \quad (4.3^a)$$

with

$$\tilde{B}(a, x | t_0, \xi, E) = \int m(w, E(t_0+a, x)) P(t_0+a, x, w | t_0, \xi, E) dw. \quad (4.3^b)$$

Note that  $\tilde{B}$  depends only on the environmental condition  $E$  prevailing between  $t_0$  and  $t_0+a$ . Also note that individuals of the same age can have different weights due to the different environments they experienced. The weight distribution of the population can be calculated from

$$n(t, x, w) = \iint b(t-a, \xi) P(t, x, w | t-a, \xi, E) da d\xi. \quad (4.4)$$

In reality the dynamics of the plant population is coupled to that of the herbivore population according to

$$\frac{\partial E(t, x)}{\partial t} = h(E(t, x)) - \int f(w, E(t, x)) n(t, w, x) dw \quad (4.5)$$

where  $h$  describes the internal dynamics of the plant population and  $f$  is the feeding rate of a herbivore of weight  $w$  at plant density  $E$ .

Now assume that  $E(t, x) = E_0$  is the (only) stable steady state of (4.5) in the absence of herbivores. Set

$$\tilde{B}_0(a, x, \xi) = \tilde{B}_0(a, x | t_0, \xi, E_0). \quad (4.6)$$

$\tilde{B}_0$  is the reproduction-and-dispersal kernel as introduced in the derivation of the linear model (section 3). When the diffusion coefficient  $s$  is independent of  $w$  and  $E$  we necessarily have

$$\tilde{B}(a, x | t_0, \xi, E) < \tilde{B}_0(a, x, \xi). \quad (4.7)$$

Furthermore the dispersal mechanism incorporated in (4.2<sup>a</sup>) is such that the influence of the environment on place  $x^*$ ,  $E(t, x^*)$ , on the contribution of some individuals to  $\tilde{B}$  becomes negligible when the distance between the place of birth of that individual and place  $x^*$  becomes large. This implies that an individual born sufficiently far into the tail of the expanding population experiences an environment near to  $E_0$  during the whole course of its life. So, let  $E(t, x) \rightarrow E_0$  for  $x \rightarrow \infty$  and all time. Then for all pairs  $(x, \xi)$  such that  $|x - \xi| < \infty$

$$\lim_{x, \xi \rightarrow \infty} \tilde{B}(t_0 + a, x | t_0, \xi, E) \rightarrow \tilde{B}_0(a, x, \xi). \quad (4.8)$$

#### Example II: A plant-pathogen system.

For an infectious plant disease the environmental variable of concern is the density of susceptible hosts,  $H(t, x)$ . The density of susceptibles does not influence the infectivity nor the dispersal of the pathogen, only the probability that an infectious unit will actually cause a new infection. This probability is

linearly proportional to the fraction of hosts still uninfected. Therefore we immediately have

$$E(t, x) = H(t, x) ,$$

$$\tilde{B}(a, x | t_0, \xi, E) = \tilde{B}(a, x, \xi) \frac{H(t_0 + a, x)}{H_0} \quad (4.9)$$

where  $H_0 = E_0$ . Using (4.9), (4.3<sup>a</sup>) holds again. The rate of change in the number of susceptibles is equal to minus the birth rate of the pathogen, therefore

$$\frac{\partial H}{\partial t} = - b(t, x).$$

This completes the specification of the plant pathogen system. This is the model investigated by Diekmann (1978). From (4.9) it is clear that (4.7) and (4.8) also hold for this example.

Using the relations (4.7) and (4.8) we now consider (4.1). Consider equation (4.3<sup>a</sup>). Relation (4.7) implies that  $b(t, x) < b^*(t, x)$ , where  $b^*$  is the solution of the linear equation (i.e. (4.3<sup>a</sup>) where  $E_0$  is substituted for  $E(\cdot, \cdot)$ ). From this one expects that the asymptotic velocity of population expansion of a non-linear model can never be larger than the asymptotic velocity of the linear model. Then (4.1<sup>a</sup>) holds with  $V(\rho)$  the minimal velocity of the linear model. Furthermore (4.8) suggests that the population dynamical behaviour of the outer part of the tail of an expanding population approaches the behaviour of the linear equation. This leads us to expect that (4.1<sup>b</sup>) holds with  $V(\rho)$  the minimal velocity of the linear model.

Generalizing from the examples and the discussion about (4.1) leads us to formulate the following conjecture:  
For any non-linear model for the autonomous spatial spread of a structured population for which (4.3<sup>a</sup>), (4.7) and an appropriate uniform version of (4.8) hold, the asymptotic velocity of population expansion is equal to the asymptotic velocity of the associated linear model obtained by setting  $E(t, x) = E_0$ .

## 5. Some numerical examples

The general linear model can be adapted to a particular species by an appropriate choice of  $\beta(a,x)$ . As an example we calculate  $C_0$  for the combination of two mechanistic models for two-dimensional rotationally symmetric dispersal densities with two descriptive models for the reproduction kernel under the assumption of statistical independence of reproduction and dispersal. Furthermore, we calculate contours of equal population density for a particular non-rotationally symmetric dispersal density.

### 5.1. Rotationally symmetric dispersal

Models for the dispersal density: In our examples we use two well-known probability densities:

i. The Gaussian density. This density arises, for example, when juveniles of a species move at random till a certain age and then settle down on a permanent breeding ground. This is the case in many sessile aquatic organisms which have swimming larvae. This dispersal density also often arises in the case of infectious diseases amongst animals, which are transmitted through physical contacts. The relative frequency with which places within a home-range of an animal are visited can often be described by a Gaussian density. Now, let an individual have the centre of its home-range at 0 and an other individual at  $x$ . The probability of encounter per unit of time then is proportional to

$$\frac{1}{(2\pi\sigma_1^2)^2} \int_{\mathbb{R}^2} e^{-\frac{|\xi|^2}{2\sigma_1^2}} e^{-\frac{|\xi-x|^2}{2\sigma_1^2}} d\xi = \frac{1}{2\pi\sigma_2^2} e^{-\frac{|x|^2}{2\sigma_2^2}} := D(x) \quad (5.1)$$

where  $\sigma_1^2$  is the variance of the Gaussian density describing the relative visiting frequency within the home range, and  $\sigma_2^2 = 2\sigma_1^2$  is the variance of the Gaussian density describing the contact rate with neighbouring individuals.

The marginal distribution is also Gaussian, with variance  $\sigma_2^2$ .

ii. The Bessel density. Assume that juveniles of a species move at random with diffusion constant  $s$ , and that they settle down at

a constant rate  $\phi$ . In a slightly different context Williams (1961) and Broadbent & Kendall (1953) showed that these assumptions lead to a distribution of settled individuals

$$D(x) = \frac{1}{4\pi\sigma_1^2} \int_0^{\infty} \frac{1}{\tau} \exp \left[ -\tau - \frac{|x|^2}{4\sigma_1^2\tau} \right] d\tau \quad (5.2^a)$$

$$= \frac{1}{2\pi\sigma_1^2} K_0 \left( \frac{|x|}{\sigma_1} \right), \quad (5.2^b)$$

where  $\sigma_1^2 = s/2\phi$  is the variance of the position of settled individuals on a line transect through the source and  $K_0$  is the modified Bessel function of the second kind of order zero.

The marginal density is the double-exponential density

$$D(x) = \frac{1}{2\sqrt{2}} \frac{1}{\sigma_2} \exp \left[ -\sqrt{2} \frac{1}{\sigma_2} |x| \right]. \quad (5.3)$$

the relation between  $\sigma_1$  en  $\sigma_2$  is

$$2\sigma_1^2 = \sigma_2^2. \quad (5.4)$$

This is also an appropriate model for the dispersal of airborne spores or seeds.

### Models for the reproduction kernel

#### i. The block-density

$$\beta^0(a) = \begin{cases} 0 & \text{for } 0 < a < a_1 \\ a_2^{-1} & \text{for } a_1 \leq a \leq a_1 + a_2 \\ 0 & \text{for } a > a_1 + a_2 \end{cases} \quad (5.5)$$

where  $a_1$  is the duration of the juvenile period, and  $a_2$  is the duration of the reproductive period. The mean,  $\mu$ , of this density is  $(a_1 + a_2)/2$ , its variance,  $v^2$ , is  $a_2^2/12$ .

#### ii. The gamma-density

$$\beta^0(a) = \frac{q(qa)^{r-1} \exp(-qa)}{\Gamma(r)}. \quad (5.6)$$

The mean,  $\mu$ , of this density is  $r/q$  and its variance,  $v^2$ , is  $r/q^2$ .

Results: In figure 3 the asymptotic wave velocity is plotted for the four special cases. In order to facilitate comparisons in



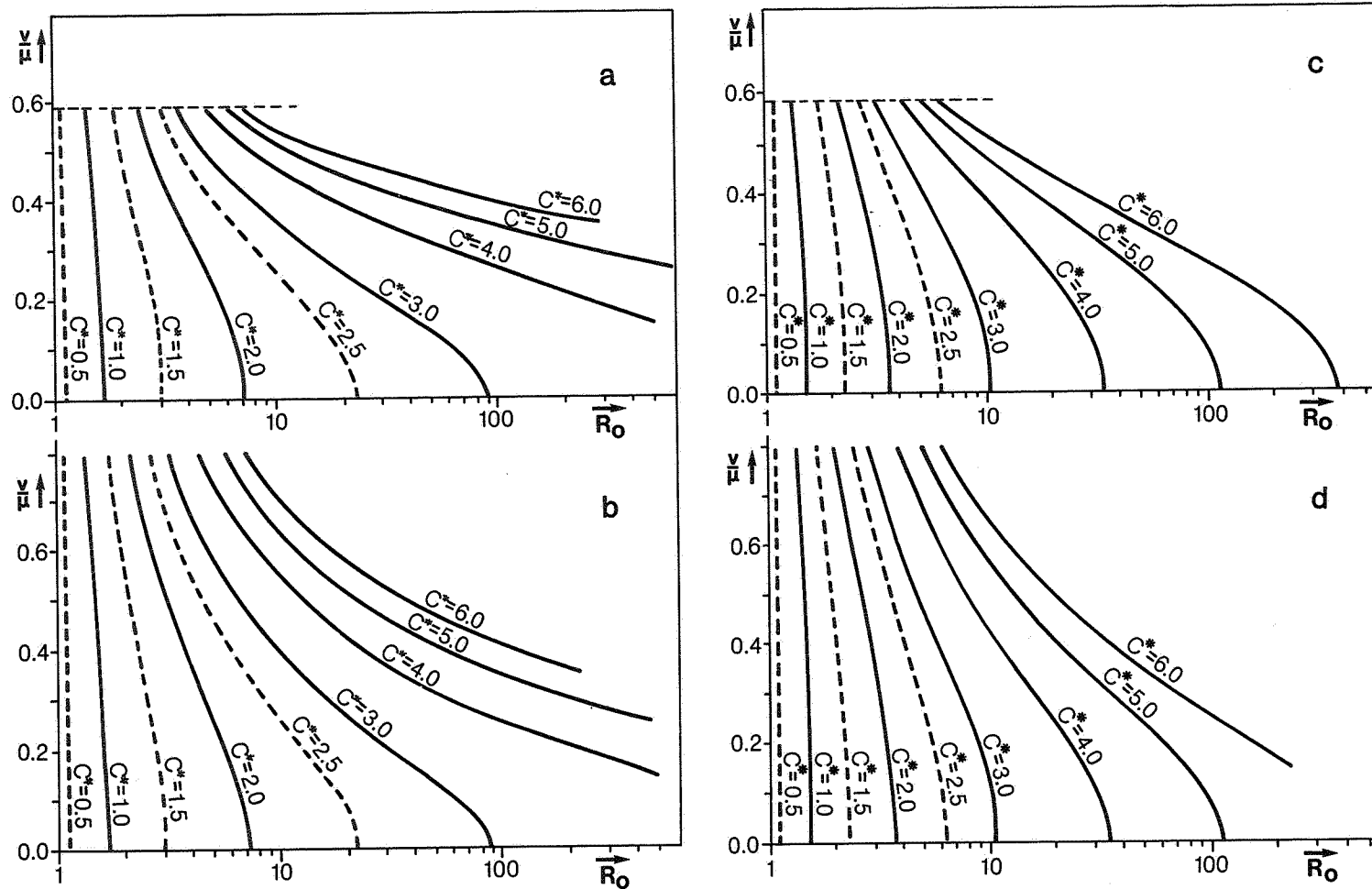


figure 3: Contour lines of the scaled wave velocity,  $C_0 = C_c \mu / \sigma$ , as a function of the net-reproduction,  $R_0$ , and the coefficient of variation,  $v/\mu$ , of the reproduction kernel,  $\sigma^2$  is the variance of the dispersal density,  $v$  and  $\mu$  are the mean and variance of the reproduction kernel. a: Block-function normalized reproduction kernel (5.5), and Gaussian dispersal density, (5.1). b: Gamma-density normalized reproduction kernel, (5.6), and Gaussian dispersal density, (5.1). c: Block-function normalized reproduction kernel, (5.5), and Bessel contact distribution, (5.3). d: Gamma-density normalized reproduction kernel, (5.6), and Bessel contact distribution, (5.3).

each case the coefficient of variation of the age-at-child bearing,  $v/\mu$ , is placed on the ordinate.

From these figures it can be seen that the wave velocity increases with increasing  $R_0$  as is to be expected. In the example with the Bessel dispersal density (fig. 3<sup>cd</sup>) the wave velocity increases approximately logarithmically with  $R_0$  (except for  $R_0$  near unity; see section 6). In the examples with a Gaussian dispersal density (fig. 3<sup>ab</sup>), however, the distance between lines of equal velocity decreases with increasing  $\ln R_0$ . This dependence can be understood by the following heuristic argument. Consider an infinitely long straight line of individuals of age zero. Their contribution to the local population density of the next generation at a distance  $x$ , is roughly proportional to  $R_0 \tilde{D}(x)$ , where  $\tilde{D}$  is the marginal-density of  $D$ . Define 'the effective distance',  $X_{\text{eff}}$ , to be the distance beyond which  $R_0 \tilde{D}(x)$  decreases below a certain number, say  $n$ . For the Bessel dispersal density

$$X_{\text{eff}} = \frac{\sigma_2}{\sqrt{2}} \ln \left[ \frac{R_0}{n} \frac{1/\sqrt{2}}{\sigma_2} \right], \quad (5.7)$$

which leads us to expect a logarithmic dependence of  $C_0$  on  $R_0$ . In the case of a Gaussian dispersal density, however,

$$X_{\text{eff}} = \sigma_2 \sqrt{2} \sqrt{\ln \left[ \frac{R_0}{n} \frac{1/\sqrt{2}}{\sigma_2 \sqrt{\pi}} \right]}, \quad (5.8)$$

explaining the observed decrease in distance between the lines of equal  $C_0$  for increasing  $R_0$ .

An other feature, which is associated with  $X_{\text{eff}}$ , is that the wave velocities for the Bessel dispersal density are larger than for the Gaussian dispersal density. The wave is dragged forward by the tail of the dispersal density. The tail of the Bessel density is thicker than the tail of the Gaussian density, or in other words if  $n \downarrow 0$ ,  $X_{\text{eff}}\text{-Bessel} > X_{\text{eff}}\text{-Gauss}$ .

When the coefficient of variation of the reproduction kernel is increased, the offspring production will start at a lower age (in the block-function case) or increase faster after  $a=0$  (in the gamma-density case). Since earlier produced offspring is longer 'put on interest' the wave velocity becomes larger with increasing coefficient of variation.

From the four examples it appears that the shape of the dispersal density is more critical to the wave velocity than the shape of the reproduction kernel. We will return to this point in section 6.

### 5.5. Non-rotationally symmetric dispersal

The dispersal density: As discussed the Bessel density is a mechanistic model describing the dispersal of spores or seeds under the influence of turbulent diffusion. Often there will also be an average displacement due to a prevailing wind direction. Assume that the wind is blowing in the  $x_2$ -direction. (5.2<sup>a</sup>) still holds in this situation if we put

$$|x| = |(x_1, x_2 - m\tau)| \quad (5.9)$$

under the integral sign where  $m$  is the average wind velocity,  $m^*$ , divided by  $\phi$ . The marginal density (3.6<sup>b</sup>) now has the form (appendix IV)

$$\tilde{D}(x) = \frac{1}{\sqrt{2}\sigma_2 \sqrt{1 + (\frac{m}{\sqrt{2}\sigma_2})^2 \sin^2 \psi}} \exp\left\{ \frac{m}{\sigma_2} \sin \psi x_1 - \frac{\sqrt{2}}{\sigma_2} |x_1| \sqrt{1 + (\frac{m}{\sqrt{2}\sigma_2})^2 \sin^2 \psi} \right\} \quad (5.10)$$

where  $\sigma_2$  is given by (5.4).

The reproduction kernel. In this example we use for the reproduction kernel a  $\delta$ -function at  $a = \mu$ .

$$\beta^0(a) = \delta(\mu) . \quad (5.11)$$

The results can be compared with the results of the rotationally symmetric Bessel-density for both reproduction kernels with  $v^2 = 0$ .

Results: In figure 4 contours of equal birth rate are plotted for some values of the net-reproduction and wind velocity. From this figure we see that for small  $R_0$  and large  $m$  no velocity of population expansion is calculated in the direction opposite to the wind direction. Too few births occur in this direction to build up a population wave and we thus have  $V < 0$ . The contours of equal population density appear to be ellipse shaped. We return to this point in section 6.

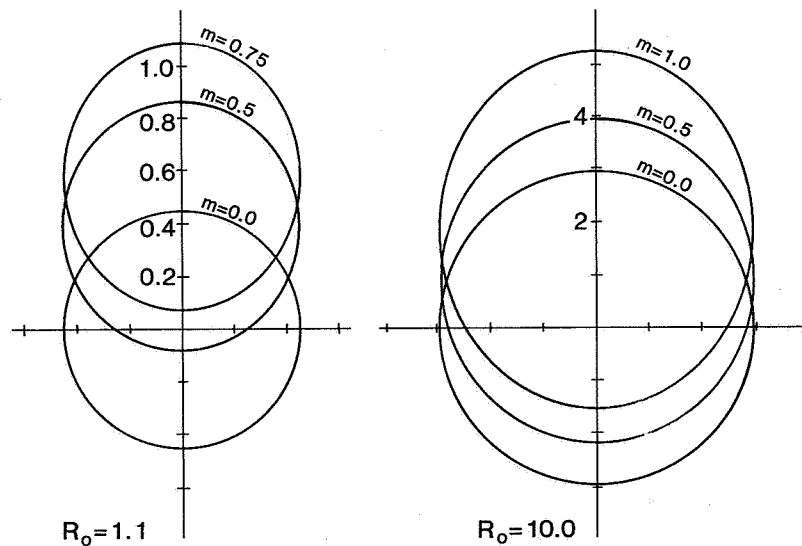


figure 4: Contours of equal birth-rate for the non-rotationally symmetric dispersal density, (5.10), and a  $\delta$ -function reproduction kernel, (5.11), for various values of the net-reproduction,  $R_0$ , and wind velocities,  $m$ .

## 6. Various approximations

For every normalized reproduction-and-dispersal kernel  $\beta(a, x)$  the associated wave velocity can be calculated numerically, as long as the transform integral (3.9) does exist. We can thus gain insight into the dependence of the wave velocity on the parameters of this specific normalized reproduction-and-dispersal kernel. It would, however, be useful to have general, preferably explicit, approximations for  $C_0$  in terms of global characteristics of the normalized reproduction-and-dispersal kernel. Such approximations may provide useful rules of thumb. Moreover, in practice, measurements of the birth kernel have a limited accuracy. This also leads us to search for methods, based on easily measurable global characteristics, from which the asymptotic wave velocity can be calculated at least to a first approximation. Finally, comparing such approximations with numerical results for specific normalized reproduction-and-dispersal kernel show to what extent  $C_0$  depends on the details of the reproduction and dispersal process.

## 6.1. Rotationally symmetric dispersal

### i. Small $R_0$

Let  $l(C, \lambda) := \ln L(C, \lambda)$ . Formula (3.9) then transforms into

$$l(C, \lambda) = \ln R_0 + \ln \int_0^{\infty} \int_{-\infty}^{\infty} e^{-\lambda(\xi+Ca)} \tilde{\beta}(a, \xi) d\xi da. \quad (6.1)$$

The second part of the right-hand side is the so-called cumulant generating function of  $\tilde{\beta}$  evaluated at  $\lambda$  and  $\lambda C$ . We shall denote the bivariate cumulants as  $\kappa_{ij}$  where the first index refers to  $\xi$  and the second to  $a$ . By definition the cumulants are the coefficients in the Taylor expansion of the cumulant generating function. Then (6.1) can be written as

$$l(C, \lambda) = \ln R_0 + \sum_{n=1}^{\infty} \sum_{i=1}^n \frac{\kappa_{n-i, i}}{(n-i)! i!} C^i (-\lambda)^n. \quad (6.2)$$

In particular

$$\kappa_{01} = \mu := \int_0^{\infty} \int_{-\infty}^{\infty} a^2 \tilde{\beta}(a, \xi) d\xi da, \quad \text{the mean age-at-child-bearing,}$$

$$\kappa_{02} = \nu^2 := \int_0^{\infty} \int_{-\infty}^{\infty} a^2 \tilde{\beta}(a, \xi) d\xi da - \mu^2, \quad \text{the variance of the age-at-child-bearing,}$$

$$\kappa_{20} = \sigma^2 := \int_0^{\infty} \int_{-\infty}^{\infty} \xi^2 \beta(a, \xi) d\xi da,$$

the variance of the (marginal density of the) places where an average female gives birth throughout its life relative to its place of birth,

$$\kappa_{ij} = 0 \text{ for } i \text{ odd, due to symmetry.}$$

Further relations between moments and cumulants may be found in Kendall & Stuart (1958). The first terms of system (3.11) become:

$$\begin{cases} 0 = \ln R_0 - \mu C \lambda + \frac{1}{2}(\sigma^2 + v^2 C^2) \lambda^2 - \frac{1}{2} \kappa_{21} C \lambda^3 - \\ \quad - \frac{1}{6} \kappa_{03} C^2 \lambda^3 + \frac{1}{24} (\kappa_{40} + 6\kappa_{22} C^2 + \kappa_{40} C^4) \lambda^4 + \dots, \\ 0 = -\mu C + (\sigma^2 + v^2 C^2) \lambda - \frac{3}{2} \kappa_{21} \lambda^2 C - \frac{1}{2} \kappa_{03} C^3 \lambda^2 \\ \quad + \frac{1}{6} (\kappa_{40} + 6\kappa_{22} C^2 + \kappa_{04} C^4) \lambda^3 + \dots \end{cases} \quad (6.3)$$

Now define  $\varepsilon^2 = \ln R_0$ , and assume that  $C_0$  and  $\lambda_0$  can be written as

$$C_0 = \alpha_1 \varepsilon + \alpha_2 \varepsilon^2 + \alpha_3 \varepsilon^3 + \dots,$$

$$\lambda_0 = \beta_1 \varepsilon + \beta_2 \varepsilon^2 + \beta_3 \varepsilon^3 + \dots$$

substitution in (6.3) and solving for subsequent  $\alpha_i$ 's and  $\beta_i$ 's leads to

$$C_0 = \frac{\sigma}{\mu} \sqrt{2 \ln R_0} [1 + \alpha \ln R_0] \quad (6.4)$$

where

$$\alpha = \left(\frac{v}{\mu}\right)^2 - \kappa_{21}/\sigma^2 \mu + \frac{1}{12} \kappa_{40}/\sigma^4$$

and

$$\lambda_0 = \frac{1}{\sigma} \sqrt{2 \ln R_0} [1 - \beta \ln R_0] \quad (6.5)$$

where

$$\beta = \left(\frac{v}{\mu}\right)^2 - 2 \kappa_{21}/\sigma^2 \mu + \frac{1}{4} \kappa_{40}/\sigma^4.$$

Note that  $\kappa_{40}$  already occurs in  $\alpha_3$  while  $\kappa_{03}$  only occurs in  $\alpha_5$ . This is consistent with the observation in section 4 that the wave velocity is more sensitive to the shape of the dispersal density than to that of the probability density of the age-at-child-bearing. In statistics  $\kappa_{40}/\sigma^4$  is called the kurtosis.

The wave velocity predicted by approximation formula (6.4) was compared with the values of the four examples from section 4. Figure 5 depicts the regions where the inaccuracy of the approximation is lower than 10% for the expansion up to order  $\varepsilon$  (i.e.  $\alpha=0$ ) and up to order  $\varepsilon^3$  (the complete formula (6.4)). It can be seen that in the case of a Gaussian contact distribution the formula is adequate even when  $R_0$  is large, provided the coefficient of variation of the probability density of the age-

at-child-bearing is small. This is due to the fact that expanding up to the second cumulant amounts to replacing the dispersal density by a Gaussian density. As expected, the parameter area where the approximation formula is accurate is larger for the expansion up to  $\epsilon^3$ .

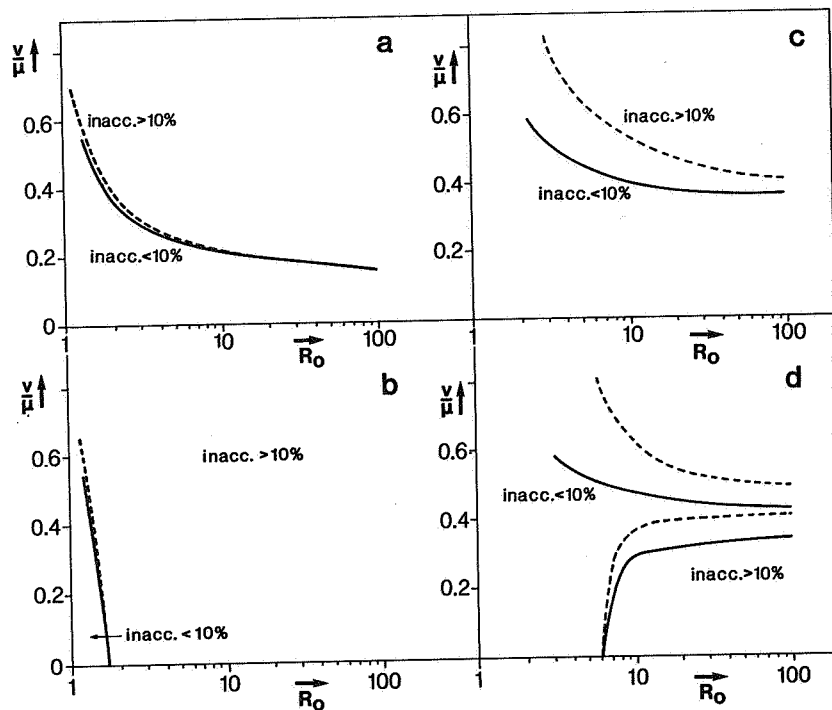


figure 5: Parameter region where the inaccuracy of the approximation formula (6.4) is less than 10%.

- a: formula (6.4) with  $\epsilon$  set equal to zero compared to the numerical examples of figure 3<sup>a</sup> and 3<sup>b</sup>.
- b: formula (6.4) with  $\epsilon$  set equal to zero compared to the numerical examples of figure 3<sup>c</sup> and 3<sup>d</sup>.
- c: formula (6.4) compared to the numerical examples of figure 3<sup>a</sup> and 3<sup>b</sup>.
- d: formula (6.4) compared to the numerical examples of figure 3<sup>c</sup> and 3<sup>d</sup>.

## ii. Concentrated reproduction kernels

The previous expansions were based on the presupposition that  $C_0$  or equivalently  $R_0 - 1$  is small. An other possibility is to consider reproduction kernels which are very concentrated. Assume, for the sake of simplicity, that  $\tilde{\beta}(a, x) = \beta^0(a) \tilde{D}(\xi)$ , and

write

$$\beta^0(a) = \varepsilon^{-1} h\left(\frac{a-\mu}{\varepsilon}\right)$$

with

$$\int_0^{\infty} ah(a) da = 0 .$$

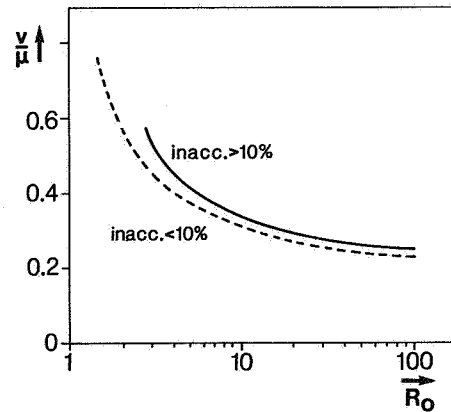


figure 6: Parameter region where the inaccuracy of approximation formula (6.6) is less than 10% compared to the numerical examples of figure 3<sup>a</sup> and 3<sup>b</sup>.

Let  $\bar{\kappa}_j$  denote the  $j^{\text{th}}$  cumulant of  $h$ . Then  $\kappa_{0j} = \varepsilon^j \bar{\kappa}_j$  and  $\kappa_{ij} = 0$  for both  $j \neq 0$  and  $i \neq 0$ . Breaking off the expansion of  $l(C, \lambda)$  after terms with  $\varepsilon^2$  yields for Gaussian  $\tilde{D}$

$$C_0 = \frac{\sigma}{\mu} \sqrt{\frac{2 \ln R_0}{1 - 2\left(\frac{v}{\mu}\right)^2 \ln R_0}} , \quad (6.6)$$

$$\lambda_0 = C_0 \frac{\mu}{\sigma^2 + (vC_0)^2} . \quad (6.7)$$

In figure 6 the predicted velocity is compared with the numerical examples with a Gaussian dispersal density. The parameter area where the inaccuracy of the approximation is lower than 10% is slightly larger than the area for the perturbation expansion up to order  $\varepsilon$ .



When the dispersal density is not Gaussian, the expansion of  $l(C, \lambda)$  in general contains infinitely many terms of order one, and we are not able to get a simple explicit expression for  $C_0$ . Yet it may be a good idea, in situations where one has a mechanistic model for the dispersal density, to derive an approximation for  $C_0$  which is based only on the mean and variance of the reproduction kernel. We shall not elaborate this any further here.

## 6.2. Non-rotationally symmetric dispersal

The starting point for the perturbation expansion is again equation (6.2).

Note that now the  $\kappa_{ij}$  depend on  $\psi$ , the angle between the direction of movement and the  $x_1$ -axis. Proceeding as before, but taking into account first order terms only, we find:

$$C_0(\psi) = \frac{\kappa_{10}}{\kappa_{01}} + \frac{\sqrt{\kappa_{01}^2 \kappa_{20} + \kappa_{10}^2 \kappa_{02} - 2\kappa_{01} \kappa_{10} \kappa_{11}}}{\kappa_{01}^2} \sqrt{2 \ln R_0}, \quad (6.8)$$

$$\lambda_0(\psi) = \left[ \kappa_{01}^2 / \sqrt{\kappa_{01}^2 \kappa_{20} + \kappa_{10}^2 \kappa_{02} - 2\kappa_{01} \kappa_{10} \kappa_{11}} \right] \sqrt{2 \ln R_0}. \quad (6.9)$$

The various cumulants now are:

$$(i) \quad \kappa_{01} = \int_0^\infty \int_{\mathbb{R}^2} a \beta(a, \xi) da d\xi := \mu,$$

the mean age at child bearing.

$$(ii) \quad \kappa_{02} = \int_0^\infty \int_{\mathbb{R}^2} a^2 \beta(a, \xi) d\xi da := v^2,$$

the variance of the age at child bearing.

$$(iii) \quad \kappa_{10} = \int_0^\infty \int_{\mathbb{R}^2} \xi \cdot v \beta(a, \xi) da d\xi := \gamma_1 \cos \psi + \gamma_2 \sin \psi$$

where

$$\gamma_i = \int_{-\infty}^\infty \xi_i \int_0^\infty \int_{\mathbb{R}^2} \beta(a, \xi) d\xi_j da d\xi_i \quad (i, j=1, 2 \text{ and } i \neq j)$$

the mean displacement in the  $x_i$ -direction of the birthplace of a child relative to that of its mother.

$$(iv) \quad \kappa_{20} = \int_0^{\infty} \int_{\mathbb{R}^2} (\xi \cdot v - \kappa_{10})^2 \beta(a, \xi) da d\xi = \sigma_{11}^2 \cos^2 \psi + 2\sigma_{12}^2 \cos \psi \sin \psi + \sigma_{22}^2 \sin^2 \psi$$

where

$$\sigma_{ij}^2 = \int_0^{\infty} \int_{\mathbb{R}^2} (\xi_i - \gamma_i)(\xi_j - \gamma_j) \beta(a, \xi) d\xi da \quad (i, j=1, 2).$$

is the covariance of the components of the displacement in the  $x_i$  direction

$$(v) \quad \kappa_{11} = \int_0^{\infty} \int_{\mathbb{R}^2} (\xi \cdot v - \kappa_{10})(a - \mu) \beta(a, \xi) d\xi da = \phi_1 \cos \psi + \phi_2 \sin \psi$$

where

$$\phi_i = \int_0^{\infty} \int_{\mathbb{R}^2} (\xi_i - \gamma_i)(a - \mu) \beta(a, \xi) d\xi da \quad (i=1, 2)$$

is the covariance of the age at childbearing and the component of the displacement in the  $x_i$ -direction. Substitution into (6.8) and rearranging yields

$$C_0(\psi) = \left( \frac{\gamma_1}{\mu} \cos \psi + \frac{\gamma_2}{\mu} \sin \psi \right) + \sqrt{2 \frac{\ln R_0}{\mu}} \cdot P(\psi) \quad (6.10^a)$$

with

$$P(\psi) = (q_{11} \cos^2 \psi + 2q_{12} \cos \psi \sin \psi + q_{22} \sin^2 \psi) \mu \quad (6.10^b)$$

and

$$q_{11} = (\mu^2 \sigma_{11}^2 + v^2 \gamma_1^2 - 2\mu \gamma_1 \phi_1) / \mu^4,$$

$$q_{12} = (\mu^2 \sigma_{12}^2 + v^2 \gamma_1 \gamma_2 - \mu(\gamma_1 \phi_2 + \gamma_2 \phi_1)) / \mu^4,$$

$$q_{22} = (\mu^2 \sigma_{22}^2 + v^2 \gamma_2^2 - 2\mu \gamma_2 \phi_2) / \mu^4.$$

This completes the derivation of the approximation formula for the velocity of plane wave solutions.

Concerning the contours of equal birth rate and the asymptotic velocity of population expansion in a certain direction from the origin,  $V(\rho)$ , we observe that equation (6.10) has the same form as equation (2.13). Combining the results of section 2 and formula (6.10) we conclude that, up to the first order in  $\varepsilon = \sqrt{\ln R_0}$ ,  $V(\rho)$  is given by equation (2.10) if we replace  $m_1$ ,  $m_2$ ,  $f(0)$ ,  $S_{11}$ ,  $S_{12}$ ,  $S_{22}$  by  $\gamma_1/\mu$ ,  $\gamma_2/\mu$ ,  $(\ln R_0)/\mu$ ,  $q_{11}$ ,  $q_{12}$ ,  $q_{22}$  respectively. In cartesian coordinates the locus of vectors

$(V(\rho) \cos \rho, V(\rho) \sin \rho)$ ,  $\rho \in [0, 2\pi)$ , is given by equation (2.9) with the same substitution.

### 6.3. Connections with the Fisher/Skellam velocity

As was discussed in section 2, diffusion models are often used in the study of invasions. The most influential (rotationally symmetric) model is that of Fisher (1937) and Skellam (1951). In this section we investigate under which conditions the asymptotic wave velocity calculated from such diffusion models is a valid approximation to the asymptotic wave velocity of the general model. In the process we also find mechanistic interpretations of the phenomenological parameters in these diffusion models. We will immediately consider the non-rotationally symmetric case, of which the 'Fisher-Skellam velocity' is a special case.

Randomly moving individuals: One of the basic assumptions of diffusion models is that an individual shows, apart from a systematic movement in a certain direction, random movement. The probability (per unit area) that an individual is at a position  $x$  when it is still alive at age  $a$ ,  $D^*(a, x | \text{alive})$ , is then given by equation (2.8) with  $f(0)=0$  and  $t$  replaced by  $a$ . The reproduction-and-dispersal kernel is obtained by multiplying  $D^*$  with the reproduction kernel  $\beta^0(a)$  defined in section 3.1. Substitution of the resulting kernel in (3.11) yields

$$\begin{cases} R_0 \int_0^{\infty} \exp \{-a (\tilde{P}(\psi) \lambda^2 + \lambda C^*)\} \beta^0(a) da = 1 \\ R_0 [2\tilde{P}(\psi)\lambda - C^*] \int_0^{\infty} \exp \{-a(\tilde{P}(\psi)\lambda^2 + \lambda C^*)\} \beta^0(a) da = 0 \end{cases} \quad (6.11)$$

where

$$C^* = C - m_1 \cos \psi - m_2 \sin \psi$$

and

$$\tilde{P}(\psi) = s_{11} \cos^2 \psi + 2s_{12} \cos \psi \sin \psi + s_{22} \sin^2 \psi.$$

It is known from mathematical demography that the intrinsic rate of natural increase,  $r$ , can be calculated from the so-called Euler-equation (Keyfitz, 1968; Roughgarden, 1979):

$$1 = R_0 \int_0^{\infty} \exp(-ra) \beta^0(a) da. \quad (6.12)$$

Rewriting (6.12) as an expression for  $R_0$  and substitution in (6.11) finally yields equation (2.13) and

$$\lambda_0(\psi) = \frac{C_0 - m_1 \cos \psi - m_2 \sin \psi}{2 \tilde{P}(\psi)}.$$

From this, we can conclude that if we identify the intrinsic rate of natural increase with  $f(0)$  the wave velocity of the general model and the diffusion model are equal irrespective of the shape of  $\beta^0(a)$ . This justifies the procedure used by, for instance, Lubina & Levin (1988) and Okubo (1986).

Slow growing populations: It is well known that the individuals of most species do not move at-random throughout their lives. When is the velocity from the diffusion model an approximation to the velocity of population expansion for such species? With the identification

$$f(0) = \frac{\ln R_0}{\mu},$$

$$\tilde{P}(\psi) = P(\psi) \quad (\text{equation 2.13 and 6.10}^b),$$

$$m_i = \frac{\gamma_i}{\mu} \quad i=1,2,$$

equation (2.13) is equal to the first term in the perturbation expansion for  $C_0$  (equation (6.10)). For the rotationally symmetric case figure 5 shows that the diffusion model velocity is a valid approximation when  $R_0$  is small, say  $R_0 \leq 1.5$ , i.e. for slow growing populations. This identification also relates the phenomenological parameters  $f(0)$ ,  $m_i$  and  $S_{ij}$  with the mechanistic parameters  $R_0$ ,  $\mu$ ,  $v^2$ ,  $\gamma_i$ ,  $\sigma_{ij}$  and  $\phi_i$ .

Remark I: The Euler-equation can be expanded in the same way as was done for the characteristic equation (3.9) in the previous section (see Metz & Diekmann, 1986, p.153-154). The lowest order term in this perturbation expansion reads  $r = \ln R_0 / \mu$  which is equal to the identification of  $f(0)$  chosen.

Remark II: On basis of the preceding discussion one might expect that any model for the spatial spread of a population can be approximated by the diffusion model provided that  $R_0 - 1 \ll 1$ , such that the population grows slowly, and we look at correspondingly large time and space scales. A more rigorous phrasing of this conjecture is given in appendix V.

## 7. Applications

In this section we show that the theory developed in the preceding sections does give quantitative predictions of the velocity of population expansion that are in good agreement with the ones observed in the field. All examples have a rotationally symmetric dispersal density. The first four examples are discussed in detail elsewhere. Only a short summary is given here. We refer to the original papers for biological and technical details. The example of rabies is treated in some detail as it has not been published elsewhere. Predicted and observed velocities of population expansion are summarized in table 1.

Table 1. The observed and predicted velocity of population expansion,  $C_0$ , for various species. (For rust and mildew the representation mean standard deviation is given.)

species	$C_0$ -observed	$C_0$ -predicted	units	% deviation
The muskrat 1900-1925	5.1	3.4	km year <sup>-1</sup>	-33
1930-1960	10.9	6.5	km year <sup>-1</sup>	-40
The collared dove	43.7	56.3	km year <sup>-1</sup>	+29
Yellow rust	9.4±0.8	8.0±1.5	cm.day <sup>01</sup>	-16
Downy mildew	2.3±0.2	3.0±2.4	cm day <sup>-1</sup>	+33
Rabies	30-60	30-40	km year <sup>-1</sup>	-

### 7.1. The muskrat (Ondatra zibethicus):

As discussed in the introduction, the muskrat started its invasion into Europe in 1905. In a recent paper Van den Bosch et al. (1988) investigate this case. They found that the velocity of population expansion before 1930 to be much larger than after

1930. This difference is probably due to the large scale trapping programs started around 1925/30.

All available literature data on the life history characteristics of the muskrat are from the period after 1930. On the basis of literature data on the age specific survivorship,  $L(a)$ , and the rate of offspring production of a female of age  $a$ ,  $m(a)$ , the net-reproduction,  $R_0$ , and the mean,  $\mu$ , and variance,  $v^2$ , of the normalized reproduction-kernel were calculated. From published capture-mark-recapture data on the dispersal of muskrats it appears that juveniles as well as adults disperse between two breeding seasons. No significant difference was found for the dispersal distance between two breeding-seasons for juveniles and adults. Using these dispersal data the variance,  $\sigma^2$ , and kurtosis of the marginal dispersal density were calculated. Luckily, the values of the parameters appeared to be in the range of applicability of approximation formula (6.4).

From the capture-mark-recapture study the mortality rate induced by the trapping program, a standard program in Europe, was calculated. Using this estimate the age specific survivorship for the period before 1930 was reconstructed and through this all other parameters recalculated. Again formula (6.4) was used to calculate the 'predicted velocity of population expansion'.

## 7.2. The collared dove (Streptopelia decaocto)

In the same paper Van den Bosch et al. (1988) also treat the invasion of the collared dove into Europe. Using literature data and additional data from the EURING data-bank on the recovery of ringed fledglings the age specific survivorship,  $L(a)$ , was constructed. Combined with literature data on the age specific reproduction rate this allowed the calculation of, the net-reproduction,  $R_0$ , and the mean,  $\mu$ , and variance,  $v^2$  of the normalized reproduction kernel.

Juveniles of the collared dove disperse and settle down definitively on a permanent breeding ground. Using the ring-recovery data mentioned gave some impression about the dispersal distance of the juveniles. The data set turned out to be too small for an estimate of the kurtosis of the marginal dispersal density to be possible. Since, however, the net-reproduction is

small ( $R_0 \approx 1,33$ ) the approximation formula (6.4) was used with  $\alpha=0$ , which corresponds to using the Fisher-Skellam velocity.

### 7.3. Yellow rust (Puccinia striiformis).

Van den Bosch et al. (1988<sup>abc</sup>) investigate the spatial development of disease foci in plant-pathogen systems. Yellow rust is a fungus living on wheat (Triticum aestivum). For this pathosystem the approximation formulae cannot be used and, in order to estimate  $C_0$ , system (3.11) was solved numerically on the basis of an appropriate sub-model for the reproduction-and-dispersal kernel.

Yellow rust is transferred between hosts by means of airborne spores. Inside the canopy layer spores move under the influence of turbulence and are trapped by infected and susceptible hosts alike. Moreover, the mean time before a spore is trapped is short relative to the time span of the infection. This implies that equation (3.4) applies. The transfer mechanism satisfies the assumptions underlying the Bessel-density (5.2). Artificial point infections were established in otherwise uninfected fields. Between 2 and 2.5 latency period after inoculation the disease severity was determined at various distances from the inoculation point. The Bessel-density was found to fit these data well.

The spore production, as a function of time since infection, of a group of lesions was measured in a growth chamber. The relative spore production as a function of the 'age-of-illness',  $\beta^0(a)$ , turned out to be well described by a gamma-density (5.6) that is shifted to account for the latency period. The latency period was obtained from the literature, and the parameters of the gamma density were estimated from the growth chamber data.

To estimate  $R_0$  artificial infections were established in a number of small wheat plots. The number of infected leaves were counted at weekly intervals. During a certain time interval the number of infected leaves increased exponentially. The rate of exponential growth,  $r$ , should satisfy (6.12). The net-reproduction,  $R_0$ , was estimated using (6.12) the estimated shifted gamma-density and the estimated  $r$ .

To test the theory artificial point infections were established in wheat fields, and the development of the foci was followed at weekly intervals.

#### 7.4. Downy mildew (Peronospora farinosa).

As a second example Van den Bosch et al. (1988<sup>C</sup>) investigated the development of downy mildew foci on spinach (Spinachia aleracea). The same procedure was followed as in the yellow rust example with one exception. Since the latency period of downy mildew lesions is approximately equal to the sporulation period of a lesion, the first few generations of an epidemic have little overlap. Therefore, the net-reproduction was estimated directly as the number of sporulating lesions of the first generation, divided by the number of sporulating zeroth generation lesions.

#### 7.5. Rabies (Lyssavirus spp.)

Rabies has been endemic in large parts of the world since historical times. Europe has been free from rabies during the last centuries. Since 1940, however, a rabies epidemic, originating from Poland, is expanding over Europe. The velocity of expansion ranges from 30 to 60 km year<sup>-1</sup>.

Rabies is characterized by a long latency period with highly variable duration and a short infective period. The infectivity during the infective period is approximately constant (Sikes, 1962). The average duration of the latency and infectious periods is approximately 35 and 5 days respectively. (Berger, 1976; MacDonald & Bacon, 1982; Bacon, 1985). If for the time being we consider  $\beta^0(a)$  to be a (deterministic) block-function then  $\mu$  equals approximately 0.1 year. This value of  $\mu$  is given by many authors (Anderson, 1982; Smith, 1985; Källén et al., 1985).

Although there seems to be consensus about the averages, very little information is available about the variability of the latency and the infective period. For the use in his stochastic simulation model, Berger (1976) constructed probability densities for the latency and infectious period on basis of a small number of experiments. Although these densities might still be far from realistic they at least give some insight. Now consider  $\beta^0(a)$  to



be a block function with a stochastic latency period,  $\underline{\ell}$ , and a stochastic infectious period,  $\underline{1}$ . In appendix VI it is shown how  $\mu$  and  $\nu$ , can be calculated for such a stochastic block function. For Berger's data

$$\mu = 33.44 \text{ days}$$

$$\nu = 4.94 \text{ days}$$

Since the coefficient of variation and  $R_0$  are both small this term is negligible in (6.4). So, our first conclusion is that detailed information about the probability density of  $\underline{\ell}$  and  $\underline{1}$  is not necessary as long as  $\mu$  is accurately determined. In the rest of our discussion we leave the coefficient of variation term out of consideration.

Andral et al. (1982) reported that three radio-tracked foxes used the same home-range before and during the period in which they were rabid. The only behavioural change appeared to be that the proportion of time spent active increased (thereby increasing the contact rate with other foxes). Therefore 'dispersal' and infectivity production are statistically independent (equation (3.4)). Consequently  $\beta$  equals zero in (6.4).

The frequency with which places in the home range are visited is well described by a two-dimensional Gaussian density (e.g. Ball, 1981). The kurtosis of a Gaussian density is zero. We are thus in a situation, where  $\alpha=0$  in (6.4). This implies that (6.4) effectively gives the Fisher/Skellam velocity. When space is completely 'filled-up' with fox home-ranges

$$\sigma^2 = \omega F^{-1} \quad (7.1)$$

where  $\sigma^2$  is the variance of the Gaussian density,  $F$  the fox population density and  $\omega$  a constant. Lambinet et al. (1978) give

$$\sigma = 2.3 \text{ km}$$

at a population density of one fox  $\text{km}^{-2}$ . So,

$$\omega \approx 5.3 .$$

Using (5.1) we find that the standard deviation,  $\sigma$ , of the marginal dispersal density is given by

$$\sigma = 10.6 F^{-1} .$$

Finally, we need information about the net-reproduction,  $R_0$ . It is obvious that  $R_0$  depends on population density. We make the assumption that

$$R_0 = E F. \quad (7.2)$$

The threshold population density,  $F_T$ , below which no rabies epidemic is possible is reported to be in the range 0.25 to 1.0 fox  $\text{km}^{-2}$  (Lloyd, 1976; Andral & Toma, 1977). The most recent, and therefore hopefully most accurate, estimate of  $F_T$  is 0.4 fox  $\text{km}^{-2}$  (Steck & Wandeler, 1980). At this threshold  $R_0=1$ , so

$$E = 2.5 \text{ km}^2 \text{ fox}^{-1}$$

Substitution of (7.1) and (7.2) in (6.4) yields

$$C_0 = \frac{\sqrt{\omega}}{\mu} \sqrt{2 \frac{\ln(EF)}{F}}. \quad (7.3)$$

The resulting relation between  $C_0$  and  $F$  is depicted in figure 7.

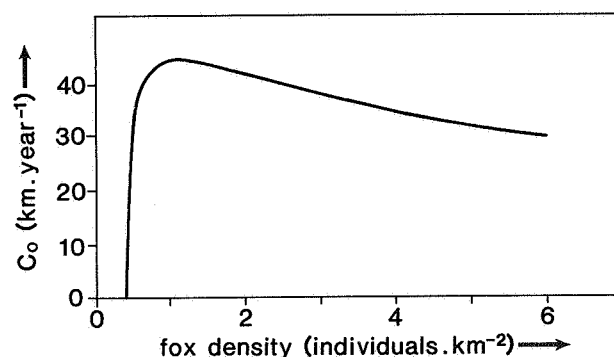


figure 7: The velocity of expansion of a rabies epidemic as a function of fox population density.

A striking feature is that intermediate velocities only occur for extremely small ranges of fox density. There is either an epidemic travelling at a, more or less, constant velocity, or there is no epidemic at all. This corresponds to observations in the field (e.g. Bögel & Moegle, 1980). An other remarkable thing is that for somewhat larger densities the velocity of rabies expansion slightly decreases with increasing fox population density. We do not know of any data confirming or falsificating this.

Källén et al. (1985) also investigate the spatial spread of rabies. They use a diffusion type model and derive a velocity equation which is basically the same as the Fisher/Skellam velocity. The (major) difference between their and our approach

is in the determination of the parameters. In our terminology Källén et al. use

$$f(0) = \frac{EF-1}{\mu}$$

which is for small  $F$  approximately equal to  $\ln(EF)/\mu$  used in (7.3). In order to estimate the diffusion coefficient  $s$  Källén et al. assume that when rabies viruses 'enter the limbic system foxes lose their sense of direction and territorial behaviour and start to wander around in a more or less random way'. This is in contradiction to the observations of Andral et al. (1982). Using this assumption  $s$  is estimated from  $S=KA$  where  $A$  is the average territory area and  $1/K$  is the average time after infection until a fox leaves its territory. A mechanistic basis for this estimation is not given. Although Källén et al. (1985) certainly gain valuable insight into the mechanisms steering the spatial spread of rabies and into control measures useful to prevent this spread, we think that in the determination of  $s$ , the problem of estimating and interpreting such phenomenological parameters becomes apparent. Due to the absence of an influence of fox density on territory size, the velocity of rabies spread as given by Källén et al. increases with population density while equation (7.3) predicts a slightly decreasing  $C_0$  at the somewhat larger population densities. It is worthwhile to confront these two opposite predictions with field data.

## 8. Discussion

We have shown how the velocity of population expansion can be calculated from knowledge of the population dynamical attributes at the individual level. Our purpose was, on the one hand, to operationalize existing theory and, on the other hand, to extend the theory into a biologically relevant direction. The indicated extensions have some open ends waiting for a mathematical analysis. Two of such open ends are presented as conjectures (section 4, appendix V).

The asymptotic result from section 3 gives us the velocity with which a population will eventually expand. It does not tell how quickly this asymptote is approached. Simulation models of

invasions usually show a rapid convergence to the 'final' velocity (Zadoks & Kampmeyer, 1977; Nobel, 1974; Ammerman & Cavali-zforza, 1984; Lubina & Levin, 1988; M. Zawolek, pers. comm.). Furthermore many real life examples also show convergence to a constant velocity within the time span of the invasion (Hengeveld in prep.; Okubo, in prep.; Van den Bosch, 1988<sup>C</sup>, in press; in prep.). Although it would be useful to have estimates on the speed of convergence, we have a gut feeling that at least the front of invading populations approaches the asymptotic velocity within an 'experimentally' reasonable time span and that the asymptotic result of section 3 can be used in many situations.

The advantage of the present approach, based on the work of Diekmann and Thieme, is that, contrary to diffusion models, hardly any assumptions are made about reproduction, survival and dispersal of individuals. About the only assumptions made are (i) the absence of Allee like effects and (ii) the presence of a sufficiently large range of population densities between the very low densities where demographic stochasticity becomes apparent; and the large densities where nonlinear effects raise their head. (See Mollison (1985,1986) for a discussion of the consequences of this last assumption being flouted.) This general approach yields a correspondingly general result about the velocity of population expansion. The real-life examples discussed in section 7 furthermore show that we have been able to catch the essentials of the processes underlying population expansion for a wide variety of species. Consequently, the way to analyzing the velocity aspect of invasions is open. Such studies are expected to give insight into the important ecological phenomenon of population expansion.

#### Acknowledgements:

We thank H.R. Thieme for organizing the Heidelberg workshop on the mathematical modelling of epidemics in November 1979. The present paper is a direct offshoot of this workshop. We are also grateful to Y. Zitman for typing the manuscript and to G.P.G. Hock for drawing the figures, and to the coauthors of our more experimentally oriented papers, J.C. Zadoks and R. Hengeveld, for discussions about the experimental application of the theoretical work developed in this paper.

## Appendix I

Derivation of (2.11) and (2.12) from (2.7)

Let

$$A = \begin{pmatrix} \cos \psi & \sin \psi \\ \sin \psi & -\cos \psi \end{pmatrix},$$

and note that  $\det A = -1$ ,  $A^{-1} = A$ . Let  $x = Ay$ . To transform (2.7) to the new coordinates  $(y_1, y_2)$  recourse is taken to the interpretation of the coefficients.  $M = (m_1, m_2)^T$  can be interpreted as the vector of infinitesimal means of the movement of the individuals, and  $S = (s_{ij})$  as the infinitesimal covariance matrix. Letting primes indicate the corresponding quantities in the  $y$ -coordinates, using the usual rules for the transformations of means and covariances gives

$$M' = AM, \quad S' = ASA^T$$

Now consider solutions which are constant in the  $(\sin \psi, -\cos \psi)$  direction, i.e. orthogonal to the  $(\cos \psi, \sin \psi)$  direction, so that  $\partial n' / \partial y_2 = 0$ . Removing all zero terms and dropping the primes and the spurious index 1 gives (2.11) and (2.12).

## Appendix II.

Transformation of (3.8) into (3.9)

The transformation equals  $\xi_1 = \xi_1' \cos \psi - \xi_2' \sin \psi$ ;  $\xi_2 = \xi_1' \sin \psi + \xi_2' \cos \psi$ . Substitution in  $\beta(a, \xi_1, \xi_2)$  yields the kernel in (3.9<sup>b</sup>). Since the Jacobean of such a rotation equals 1 and

$$\xi \cdot v = \xi_1 \cos \psi + \xi_2 \sin \psi =$$

$$\xi_1' \cos^2 \psi - \xi_2' \sin \psi \cos \psi + \xi_1' \sin^2 \psi + \xi_2' \sin \psi \cos \psi =$$

$$= \xi_1'$$

we arrive at (3.9<sup>a</sup>).

## Appendix III.

The relation between  $V(\rho)$  and  $C_0(\psi)$ 

Let  $V(\rho)$  be the asymptotic velocity of population expansion in the  $\rho$  direction, i.e.

$$\lim_{t \rightarrow \infty} b(t, ty) = \begin{cases} 0 & \text{for all } y \text{ outside } A \\ \infty & \text{for all } y \text{ inside } A \end{cases} \quad (\text{III.1})$$

where

$$A = \{V(\rho) \begin{pmatrix} \cos \rho \\ \sin \rho \end{pmatrix} : \rho \in [0, 2\pi)\} \quad (\text{III.2})$$

Let  $C_0(\psi)$  be the minimal wave speed in the direction  $\psi$ . We expect that asymptotically the expansion is governed by plane waves in all directions and that, therefore, a consistency relation between  $V(\rho)$  and  $C_0(\psi)$  must hold. We first present a formal, local and geometrical derivation of this condition. Next we turn to a result of Weinberger (1983) about the relation between  $V(\rho)$  and  $C_0(\psi)$  in his discrete time model.

Assume that  $V(\rho)$  is a smooth function of  $\rho$ . Now, consider figure 8. Translate the intersection point  $(x, y)$  to the origin and rotate the figure over  $\frac{1}{2}\pi - \psi$ . The contour can, due to our smoothness assumption, locally be approximated by

$$y = -ax^2 + o(x^2)$$

Now let  $\theta(x)$  be the angle with the  $x$ -axis of the normal to the contour at point  $x$  (figure 8<sup>b</sup>). Then

$$\theta = \frac{1}{2}\pi + \arctan(-2ax) = \frac{1}{2}\pi - 2ax + o(x^3)$$

In a small timestep  $\Delta$  the contour is at most  $O(\Delta)$  translated, so we can restrict to  $x$ 's of this order. In the timestep  $\Delta$  the point  $(x, y)$  on the contour is translated to:

$$\begin{aligned} (\bar{x}, \bar{y}) &= (x + C(\psi + \theta - \frac{\pi}{2}) \cos(\theta)\Delta; y + C(\psi + \theta - \frac{\pi}{2}) \sin(\theta)\Delta) \\ &\approx (x + C(\psi - 2ax)2ax\Delta; y + C(\psi - 2ax)\Delta) \end{aligned}$$

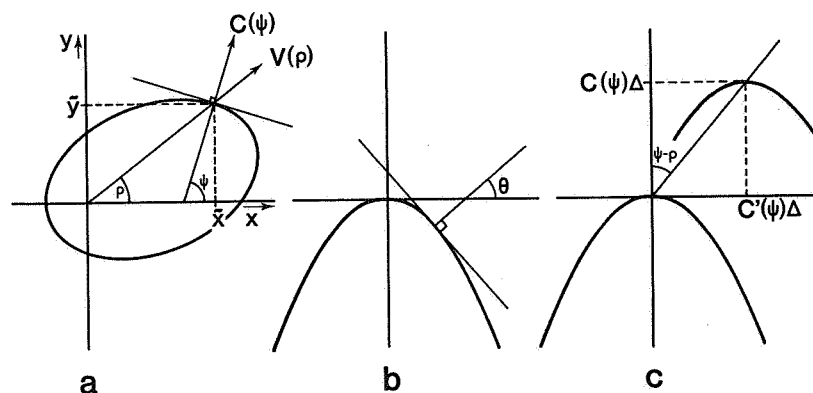


figure 8: see the text.

So, the translated contour is up to second order terms given by

$$y = -ax^2 + C(\psi - 2ax)\Delta \approx -ax^2 - C'(\psi) 2ax\Delta + C(\psi)\Delta$$

(see figure 8<sup>C</sup>), and the new top of the parabola is now

$$(\bar{x}, \bar{y}) = (-C'(\psi)\Delta ; C(\psi)\Delta)$$

which finally leads to

$$\psi - \rho = \arctan \left( -\frac{C'(\psi)}{C(\psi)} \right)$$

$$V(\rho) = \sqrt{(C(\psi))^2 + (C'(\psi))^2}$$

or equivalently equation (3.12).

Weinberger (1983) has derived the characterization

$$A \hat{=} \{x : x_1 \cos \psi + x_2 \sin \psi \leq c_0(\psi) \text{ for all } \psi \in [0, 2\pi)\} \text{ (III.3)}$$

in the context of a discrete time model. Combining (III.2) and (III.3) we find

$$V(\rho) \cong \frac{C_0(\psi)}{\cos(\psi-\rho)} := F_\rho(\psi), \text{ for all } \psi \in [0, 2\pi). \quad (\text{III.4})$$

If  $x$  is a point of the boundary separating the 'inside' from the 'outside' of the set it necessarily satisfies

$$V(\rho) = \min_{\psi} F_\rho(\psi) \quad (\text{III.5})$$

or similarly

$$\frac{dF_\rho}{d\psi} = 0 ; V(\rho) = F_\rho(\psi) \quad (\text{III.6})$$

which, in its turn, equals (3.12).

Inequality (III.4) is more restrictive than (III.5). What then is the difference between (3.12) and the Weinberger result? To answer this question consider the function  $F_\rho(\psi)$ . Note that for  $(\psi-\rho) \rightarrow \frac{1}{2}\pi$ ,  $F_\rho(\psi) \rightarrow \infty$ . Using the first equation of (III.6) we possibly find, besides the absolute minimum, one or more local minima and maxima. If such a local minimum exist it can if we gradually change  $\rho$  : (a) disappear because the local minimum and maximum fuse, (b) become the absolute minimum leaving the former absolute minimum as local minimum, or (c) a combination of these two. Combining this with the second equation of (III.6) it can be seen that the graph of  $V(\rho)$  consists, at least, of a closed curve resulting from the absolute minimum (the AMCC). The local minima/maxima could possibly cause isolated closed curves 'outside' the AMCC, loops on the 'outside' of the AMCC fusing with the AMCC at one point, or more exotic possibilities like double loops in conjunction with closed curves, etc. The important point is that the properties of  $F_\rho(\psi)$  mentioned ensure that loops and isolated closed curves cannot occur 'inside' the AMCC. The closed convex set  $A$  as given by Weinberger equals the AMCC leaving out the isolated closed curves and pruning the loops. This pruning may result in a sharp angle. It are such sharp angles where the geometrical derivation breaks down.

In conclusion we can say that equation (3.12) tells the whole story if  $V(\rho)$  is a smooth function of  $\rho$ , which is biologically reasonable. In other situations (3.12) also gives us the desired contour of equal birth rate/population density after pruning of



loops and crossing out isolated islands. Whether or not such loops or islands do actually occur for 'decent' kernels we don't know.

#### Appendix IV

##### Derivation of formula (5.10)

The dispersal density takes the form

$$D(x_1, x_2) = \frac{1}{4\pi\sigma_1^2} \int_0^{\infty} \frac{1}{\tau} \exp \left[ -\tau - \frac{x_1^2 + (x_2 - m\tau)^2}{4\sigma_1^2 \tau} \right] d\tau$$

Substitution of  $x_1' = x_1 \cos \psi + x_2 \sin \psi$ ;  $x_2' = -x_1 \sin \psi + x_2 \cos \psi$  and dropping the primes again yields

$$D(x_1, x_2) = \frac{1}{4\pi\sigma_1^2} \int_0^{\infty} \frac{1}{\tau} \exp \left[ -\tau - \left( \frac{1}{4\sigma_1^2} \right) \left( \frac{x_1^2}{\tau} + \frac{x_2^2}{\tau} - 2m(x_1 \sin \psi + x_2 \cos \psi) + m^2 \tau \right) \right] d\tau$$

The marginal density is found from

$$\tilde{D}(x_2) = \int_{-\infty}^{\infty} D(x_1, x_2) dx_1$$

We first calculate

$$\int_{-\infty}^{\infty} \exp \left\{ -\frac{1}{4\sigma_1^2} \left( \frac{x_2^2}{\tau} - 2m \cos \psi x_2 \right) \right\} dx_2$$

Using Siegel (1968, p.98, formula 15.75) this integral equals

$$\sqrt{4\pi\sigma_1^2 \tau} \exp \left\{ \left( \frac{m \cos \psi}{2\sigma_1} \right)^2 \tau \right\}$$

So,

$$\tilde{D}(x_1) = \alpha \int_0^{\infty} \frac{1}{\sqrt{\tau}} \exp \left\{ -\left\{ \beta \tau + \gamma \frac{1}{\tau} \right\} \right\} d\tau$$

where

$$\alpha = \frac{1}{2\sigma_1 \sqrt{\pi}} \exp \left\{ \frac{m \sin \psi}{2\sigma_1} x_1 \right\}$$

$$\beta = 1 + \left( \frac{m}{2\sigma_1} \right)^2 \sin^2 \psi$$

$$\gamma = \left( \frac{x_2}{2\sigma_1} \right)^2$$

Substitution of  $\tau' = \sqrt{\tau}$  and dropping the primes gives

$$\tilde{D}(x_1) = \alpha \cdot 2 \int_0^{\infty} \exp - \left\{ \beta \tau^2 + \gamma \frac{1}{\tau^2} \right\} d\tau$$

Using Siegel (1968, p.98, formula 15.78) we find

$$\tilde{D}(x_1) = \alpha \sqrt{\frac{\pi}{\beta}} \exp\{-2 \sqrt{\beta\gamma}\}$$

So,  $\tilde{D}(x_1)$  is indeed given by formula (5.10). The Laplace transform

$$L\{\tilde{D}(x_1), \lambda\} = \int_{-\infty}^{\infty} e^{-\lambda x_1} \tilde{D}(x_1) dx_1$$

is easily calculated to be

$$\frac{1}{1 + m \lambda \sin \psi - \frac{\lambda^2 \sigma_2^2}{2}}$$

#### Appendix V

##### A further connection with the Fisher/Skellam model

In section 6 it was shown that the velocity of population expansion, as calculated from the Fisher/Skellam model, is, if we make the right identification between the model parameters, equal to the lowest order term of the approximation formula derived from a perturbation expansion. Considering the parameter region where this approximation formula is valid leads us to expect that when

$$\ln R_0 \downarrow 0, \quad \mu \downarrow 0, \quad \sigma^2 \downarrow 0$$

in such a way that  $\ln R_0/\mu$  and  $\sigma^2/\mu$  remain constant, the Fisher/Skellam model is an approximation to the general model. Before formulating such a conjecture we make some preliminary remarks about non-spatial models.

The state  $N$  of a, non-spatial, general structured population model always satisfies an equation

$$\frac{dN}{dt} = A_{\theta}(E)N \quad (V.1)$$

with  $A_{\theta}(E)$  a linear operator depending on the environment  $E$ , where  $E(t) \in \mathbb{R}^k$ . The parameter  $\theta$  is introduced for convenience to be used later on. For constant environment,  $E(t) = \tilde{E}$ , we assume that  $A$  depends on  $E$  and  $\theta$  in such a way that the corresponding semigroups are uniformly continuous in  $E$  and  $\theta$ . Denote by  $\lambda_d(A_{\theta}(\tilde{E}))$  the right-most (dominant) eigenvalue of  $A_{\theta}(\tilde{E})$ .

Environmental feedback is either direct, i.e.,  $E = G(HN)$  where  $H$  is a linear operator with finite dimensional range, or indirect through an equation of the form

$$\frac{dE}{dt} = F(E, HN) \quad (V.2)$$

In the second case we assume that for fixed  $HN = Y$  there is a unique globally stable steady-state  $\hat{E}$  of (V.2) given by  $\hat{E} = G(Y)$  with  $G$  continuous. Let  $E_0 := G(0)$ .

Assume, for simplicity, that everyone is born equal. We can then define  $R(A_{\theta}(\tilde{E}))$  to be the total expected lifetime offspring number under constant environmental condition  $\tilde{E}$ , as in section (3.1), and  $\mu(A_{\theta}(\tilde{E}))$  to be the mean age-at-childbearing (section 6.1). Note that in this situation an age representation of (V.1) is possible (for an example see section 4).

The parameter  $\theta$  is incorporated in  $A_{\theta}$  such that for  $\theta \downarrow 0$  we have

$$A_{\theta}(E) \rightarrow \bar{A} \quad (V.2^a)$$

with

$$\lambda_d(\bar{A}) = 0 = R(\bar{A}) - 1, \quad (V.2^b)$$

such that  $\bar{A}$  is not degenerated (that is to say the corresponding birth-kernel is not a single  $\delta$ -function).

Denote by  $\tilde{N}$  the (unique) eigenvector of  $\bar{A}$  corresponding to  $\lambda_d(\bar{A}) = 0$ , and by  $v$  the corresponding eigenvector of the adjoint of  $\bar{A}$ , normalized such that

$$\langle v, \tilde{N} \rangle = 1$$

$\tilde{N}$  can be interpreted as the stable  $i$ -state distribution of the population and  $v$  is the reproductive value as a function of the  $i$ -state.

For  $\theta \ll 1$ , or correspondingly  $R(A_\theta(\tilde{E})) - 1 \ll 1$ , the dominant eigenvalue of  $A_\theta(\tilde{E})$  can be approximated by

$$\lambda_d(A_\theta(\tilde{E})) \approx \frac{R(A_\theta(\tilde{E})) - 1}{\mu(\bar{A})} \quad (V.3)$$

The quantity  $1/\lambda_d$  is a measure of the timescale of population growth. For  $\theta \downarrow 0$ , population growth becomes extremely slow, so that the timescale of convergence to the stable  $i$ -state distribution is fast relative to any change in the individuals reproduction and survival due to changing input conditions. This timescale argument leads us to expect that for  $\theta \downarrow 0$  and looking at the right timescale, which will be defined below,  $N \rightarrow n\tilde{N}$  where  $n$  is a function of time only, representing the population density. Moreover, the environment will always be approximately in its steady state,  $\tilde{E} = G(nH\tilde{n})$ .

For infinitesimally small  $\theta$  we would have to wait infinitely long before we see any change in population density. To account for this problem we scale the time by introducing

$$\tau = E(\theta)t, \quad (V.4^a)$$

where

$$E(\theta) = \frac{R(A_\theta(E_0)) - 1}{\mu(\bar{A})}, \quad (V.4^b)$$

the per capita population growth rate at infinitesimally small population density.

The above discussion leads us to the following

Conjecture I: Any model for the growth of a structured population can, given all assumptions made in the preceding discussion, be approximated by

$$\frac{dn}{d\tau} = f(n) n,$$

with initial condition  $n(0) = \langle v, N(0) \rangle$ , and

$$f(n) = \lim_{\theta \downarrow 0} \frac{R(A_\theta(G(nH\tilde{n}))) - 1}{R(A_\theta(E_0)) - 1}, \quad (V.6)$$

provided that this limit exists.

Now add a spatial dimension to the model. (V.1) and (V.2) become

$$\frac{\partial N}{\partial t}(t, x) = a_{\theta}(E)N \quad (V.7)$$

$$\frac{\partial E}{\partial t}(t, x) = \bar{U}(E, HN)$$

The linear operator  $a_{\theta}$ , for which we make the same assumptions as for  $A_{\theta}$ , now incorporates both the demographic and the dispersal characteristics. We also assume  $a_{\theta}(E)$  to be such that

$$[E(t, x) = E^*(t) \text{ and } N(t, x) = N^*(t)] \Rightarrow a_{\theta}(E) = A_{\theta}(E) \quad (V.8)$$

Again  $\theta$  is incorporated in  $a_{\theta}$  such that for  $\theta \downarrow 0$ ,  $a_{\theta}(E) \rightarrow \bar{a}$  with  $\lambda_d(\bar{a}) = 0$ . Again  $\bar{a}$  is not degenerate (in time and space).

We assume that the initial condition is sufficiently smooth in time (age) and space. Again for  $\theta \downarrow 0$  the local rate of population growth and the rate of change of the environment, is extremely slow. This causes the profile (in the  $x$ -direction) of population densities and the profile of the environmental variable to be extremely flat. In the limit for  $\theta \downarrow 0$  every individual will experience an environment which is constant in space, i.e.  $E(t, x) = E(t)$ . Assumption (V.8) therefore makes that the local rate of population growth can again be approximated by (V.3).

In the limit for  $\theta \downarrow 0$ ,  $R(\bar{a}) = 1$  so every individual just replaces itself. Every individual produces one offspring at a random age. This age is drawn from the reproduction kernel, as defined in section 3. The place of birth of this child is also a random variable drawn from the dispersal density  $D(x)$ , as defined in section 3. Therefore on the timescale of population change the individuals perform a random walk. The rate of increase of the variance per generation, the diffusion coefficient  $S$ , can be approximated by

$$S = \frac{1}{2} \frac{\sigma^2}{\mu(\bar{A})}, \quad (V.9)$$

where  $\sigma^2$  is the variance of  $D(x)$ .

Collecting all results from the above discussion we can formulate the following

Conjecture II: Any model for the spatial spread of a structured population can, given all assumptions made in the preceding discussion, be approximated by the Fisher/Skellam diffusion equation (2.1)

$$\frac{\partial n}{\partial t} = S \frac{\partial^2 n}{\partial x^2} + f(n) n$$

where  $f(n)$  is given in (V.6) and  $S$  in (V.9).

## Appendix VI

### The mean and variance of a stochastic block function

In this appendix we show how the mean and variance of the reproduction kernel can be calculated for a stochastic block function. Since these calculations are used in the rabies example we use the terminology of infectious diseases.

Consider a block-function with a stochastic latency period ( $\underline{\ell}$ ), a stochastic infective period ( $\underline{l}$ ) and a stochastic infectiousness ( $\underline{\zeta}$ ). When  $\underline{\ell}$  and  $\underline{l}$  are independent variables respectively with probability density  $f_{\ell}$  and survivor function  $\mathcal{F}_l$ , the average infectiousness of an individual  $\tau$  time after infection is

$$i(\tau) = (\mathcal{E}[\underline{l}])^{-1} \int_0^{\tau} f(x) \mathcal{F}_l(\tau-x) dx$$

This model subsumes the usual two stages (latent and infective) differential equation models in which both  $f_{\ell}$  and  $\mathcal{F}_l$  are assumed to be exponential. The two special time kernels from section 4, the block and gamma kernels, can be derived from it by assuming the densities of  $\underline{l}$  and  $\underline{\ell}$  to be respectively both degenerated and gamma ( $\rho-1, \ell$ ) and exponential ( $\ell$ ).

The mean and variance of  $i(\tau)$  can be calculated as follows. The mean infectivity of an individual is given by

$$I(\tau) = \mathcal{E}[\eta(\tau)],$$

where the individual infectivity  $\eta$  equals

$$\eta(\tau) = \underline{\zeta} \{ H(\tau - \underline{\ell}) - H(\tau - \underline{\ell} - \underline{l}) \}$$

with  $H$  the Heaviside-step-function. And

$$\gamma = \int_0^{\infty} I(\tau) d\tau = \mathcal{E} \left[ \int_{\underline{\ell}}^{\underline{\ell} + \underline{l}} \eta(\tau) D\tau \right] = \mathcal{E}[\underline{\zeta} \underline{l}].$$

By definition  $i(\tau) = \frac{\ell}{\gamma} I(\tau)$ . The mean,  $\mu$ , of the time kernel is found from

$$\mu = \int_0^{\infty} \tau i(\tau) d\tau = \gamma^{-1} \left[ \int_0^{\frac{\ell+1}{\ell}} \tau \eta(\tau) d\tau \right] = \frac{\mathcal{E}[\underline{\ell} \underline{\zeta}] + \frac{1}{2} \mathcal{E}[\underline{\zeta} \underline{\ell}^2]}{\mathcal{E}[\underline{\zeta} \underline{\ell}]}$$

When  $\underline{\ell}$ ,  $\underline{\ell}$  and  $\underline{\zeta}$  are independent

$$\mu = \mathcal{E}[\underline{\ell}] + \frac{1}{2} \mathcal{E}[\underline{\ell}] (1 + C^2[\underline{\ell}]), \quad (\text{VI.1})$$

where  $C[\underline{\ell}]$  is the coefficient of variation of  $\underline{\ell}$ . The calculation of the variance,  $\sigma^2$ , precedes along the same lines

$$\mu^2 + \nu^2 = \int_0^{\infty} \tau^2 I(\tau) d\tau = \gamma^{-1} \mathcal{E} \left[ \int_0^{\frac{\ell+1}{\ell}} \tau^2 \eta(\tau) d\tau \right] = \frac{\mathcal{E}[\underline{\zeta} \underline{\ell}^2 \underline{\ell}] + \mathcal{E}[\underline{\zeta} \underline{\ell} \underline{\ell}^2] + \frac{1}{3} \mathcal{E}[\underline{\zeta} \underline{\ell}^3]}{\mathcal{E}[\underline{\zeta} \underline{\ell}]}$$

And under the independence assumption,

$$\nu^2 = \text{var.}[\underline{\ell}] + \frac{1}{2} \text{var}[\underline{\ell}] (1 - \frac{1}{2} C^2[\underline{\ell}]) + (\mathcal{E}[\underline{\ell}])^2 \left( \frac{1}{12} + \frac{1}{3} S[\underline{\ell}] C^3[\underline{\ell}] \right), \quad (\text{VI.2})$$

where  $S[\underline{\ell}]$  is the skewness of  $\underline{\ell}$ .

(VI.1) and (VI.2) relate the quantities used in section 5 to quantities which are sometimes slightly better known. Usually we can make fair guesses about the mean and variance of the latency period. (VI.1) and (VI.2) moreover show that contrary to the situation for the contact distribution in the case of the time kernel an approach based on a direct phenomenological measurement may be preferable to an approach based on detailed micromodels. A quantity like the skewness of the infective period,  $S[\underline{\ell}]$ , is difficult to measure. Yet this quantity occurs already in the expression for the variance,  $\nu^2$ , of the time kernel.

For the probability density given by Berger (1976) we find

$$C(\underline{\ell}) = 0.32 \quad ; \quad \mathcal{E}(\underline{\ell}) = 2.99 \quad ; \quad \mathcal{E}(\underline{\ell}) = 7.9 \quad ;$$

$$\text{var}(\underline{\ell}) = 14.08 \quad ; \quad \text{var}(\underline{\ell}) = 6.47 \quad ; \quad S(\underline{\ell}) = 2.96$$

### References

1. Ammerman, A.J., Cavalli-Sforza, L.L.: The neolithic transition and the genetics of populations in Europe. Princeton University Press 1984.
2. Anderson, R.M. (ed.): Population dynamics of infectious diseases; Theory and applications. London: Chapman & Hall 1982.

3. Andral, L., Artois, M., Aubert, M.F.A., Blancou, J.: Radiopistage de renards enrages. *Comp. Immunol. Microbiol. Infect. Diseases* **5**, 284-291 (1982)
4. Andral, L., Toma, B.: La rage en France en 1976. *Rec. Med. vet.* **153**, 503-508 (1977)
5. Anonymous: Ecology of biological invasions. *SCOPE Newsletter* **23**, 1-5 (1985)
6. Aronson, D.G., Weinberger, H.F.: Nonlinear diffusion in population genetics, combustion, and nerve pulse propagation. In: Goldstein, J.A. (ed.) *Partial differential equations and related topics*. (Lect. Notes Math., vol. 446, pp. 5-49) Berlin: Springer 1975.
7. Aronson, D.G., Weinberger, H.F.: Multidimensional nonlinear diffusion arising in population genetics. *Adv. in Math.* **30**, 33-76 (1978)
8. Bacon, P.J. (ed.): *Population dynamics of rabies in wildlife*. Academic Press 1985
9. Ball, F.G.: Some statistical problems in the epidemiology of fox rabies. Thesis 302 pp. 1981
10. Berger, J.: Model of rabies control. In: Berger, J., Buhler, W., Reppes, R., Tautu, P. (eds.) *Mathematical models in medicine*. (Lect. Notes Biomath., vol. 11, pp. 75-88) Berlin, Springer 1976
11. Bögel, K., Moegle, H.: Characteristics of the spread of a wildlife rabies epidemic in Europe. *Biogeographica* **8**, 251-258 (1980)
12. Bramson, M.: Convergence of solutions of the Kolmogorov equation to travelling waves. *Memoir of the American Mathematical Society* **44**, no. 285, 190 pp. (1983).
13. Broadbent, S.R., Kendall, D.G.: The random walk of *Trichosporonyx retortaeformis*. *Biometrika* **9**, 460-465 (1953)
14. Caughley, G.: Liberation, dispersal and distribution of Himalayas Thar (*Hemitragus jemlahicus*) in New Zealand. *New Zealand Journal of Science* **13**, 220-239 (1970)
15. Creegan, P., Lui, R.: Some remarks about the wave speed and travelling wave solutions of a nonlinear integral generator. *J. Math. Biology* **20**, 59-68 (1984)
16. Diekmann, O.: Thresholds and travelling waves for the geographical spread of infection. *Journal of Mathematical Biology* **6**, 109-130 (1978)
17. Diekmann, O.: Run for your life. A note on the asymptotic speed of propagation of an epidemic. *Journal of Differential Equations* **33**, 58-73 (1979)
18. Diekmann, O.: Dynamics in biomathematical perspective. In: Hazewinkel, M., Lenstra, J.K., Meertens, L.G.L. (eds.) *Mathematics and computer science II*. (CWI Monographs vol.4, pp.23-50) 1986
19. Diekmann, O., Temme, N.M.: *Nonlinear diffusion problems*. Amsterdam, Mathematical Centre 247pp. 1976
20. Fisher, R.A.: The wave of advance of advantageous genes. *Ann. Eugen.* **7**, 355-369 (1937)
21. Hadeler, K.P., Rothe, F.: Travelling fronts in nonlinear diffusion equations. *J. Math. Biol.* **2**, 251-263 (1975)
22. Hengeveld, R.: *Mechanisms of biological invasions*. London: Chapman and Hall, in press
23. Källen, A., Arcuri, P., Murray, J.D.: A simple model for the spatial spread and control of rabies. *Journal of Theoretical Biology* **116**, 377-393 (1985)



24. Kendall, M.G., Stuart, A.: The advanced theory of statistics, Vol. I. London: Charles Griffin & Company Ltd. 1958
25. Kendall, D.G.: Mathematical models of the spread of infection. In: Mathematics and computer science in biology and medicine (Medical Research Council, London, 213-224) 1965
26. Keyfitz, N.: Introduction to the mathematics of population. Massachusetts: Addison Wesley Publ. Comp. 1968
27. Kolmogorov, A., Petrovsky, I., Piscounov, N.: Etude de l'équation de la diffusion avec croissance de la quantité de matière et son application a un problème biologique. Moscou Universitet. Bull. Math. 1, 1-25 (1937)
28. Lambinet, D., Boisvieux, J.F., Mallet, A., Artois, M., Andral, L.: Modèle mathématique de la propagation d'une épizootie de rage vulpine. Rev. Epidém. et Santé Publ. 26, 9-28 (1978)
29. Lloyd, H.G.: Wildlife rabies in Europe and the British situation. Trans. R. Soc. Trop. Med. Hyg. 70, 179-187 (1976)
30. Lubina, J.A., Levin, S.A.: The spread of a reinvading species: Range expansion in the California Sea Otter. Am. Nat. 131, 526-543 (1988)
31. MacDonald, D.W.: Rabies and wildlife. Oxford: Oxford University Press 1980
32. MacDonald, D.W., Bacon, P.J.: Fox society, contact rate and rabies epizootiology. Comp. Immunol. Microbiol. Infect. Dis. 5, 247-256 (1982)
33. Metz, J.A.J., Diekmann, O.: The dynamics of physiologically structured populations. Lecture Notes in Biomathematics, Vol. 68. Berlin: Springer Verlag, 511 pp. 1986
34. Mollison, D.: The rate of spatial propagation of simple epidemics. In: Le Cam, L.M., Neyman, J., Scott, E.L. (eds.) Proc. Sixth Berkeley Symposium, III, Univ. of California Press, 579-614. 1972
35. Mollison, D.: Spatial contact models for ecological and epidemic spread. J. Roy. Statist. Soc. B39, 283-326 (1977)
36. Mollison, D., Kuulasmaa, K.: Spatial epidemic models: theory and simulations. In: Bacon, (ed.) Population dynamics of rabies in wildlife, 291-309 Academic Press 1985
37. Mollison, D.: Modelling biological invasions: chance, explanation, prediction. Philosophical transactions of the Royal Society of London, series B, 314, 675-693.
38. Mood, A.M., Graybill, F.A., Boes, D.C.: Introduction to the theory of statistics. MacGraw-Hill 1974
39. Niewold, F.J.J.: Irregular movements of the red fox (*Vulpes vulpes*), determined by radio tracking. XIth International congress of game biology. RIN-mededelingen no. 84 331-337. Stockholm Sept. 1973
40. Nobel, J.V.: Geographic and temporal development of plagues. Nature 250, 726-729 (1974)
41. Okubo, A.: Diffusion-type models for avian range expansion. Preprint 1986
42. Roughgarden, J.: Theory of population genetics and evolutionary ecology: an introduction. New York: MacMillan 1979
43. Siegel, M.R.: Mathematical handbook. Schaum's outline series. McGraw-Hill 1968
44. Sikes, R.K.: Pathogenesis of rabies in wildlife. I. Comparative effect of varying doses of rabies virus inoculated into foxes and skunks. Am. J. Vet. Res. 23, 1041-1047 (1962)

45. Skellam, J.G.: Random dispersal in theoretical populations. *Biometrika* **38**, 196-218 (1951)
46. Smith, A.D.M.: A continuous time deterministic model of temporal rabies. In: Bacon, P.J. (ed.) *Population dynamics of rabies in wildlife*. Academic Press 1985
47. Steck, F., Wandeler, A.: The epidemiology of fox rabies in Europe. *Epidemiol. Rev.* **2**, 71-96 (1980)
48. Thieme, H.R.: A model for the spatial spread of an epidemic. *Journal of Mathematical Biology* **4**, 337-351 (1977<sup>a</sup>)
49. Thieme, H.R.: The asymptotic behaviour of solutions of nonlinear integral equations. *Mathematisches Zeitschrift* **157**, 141-154 (1977<sup>b</sup>)
50. Thieme, H.R.: Asymptotic estimates of the solutions of nonlinear integral equations and asymptotic speeds for the spread of populations. *Journal für die reine und angewandte Mathematik* **306**, 94-121 (1979<sup>a</sup>)
51. Thieme, H.R.: Density-dependent regulation of spatially distributed populations and their asymptotic speed of spread. *Journal of Mathematical Biology* **8**, 173-187 (1979<sup>b</sup>)
52. Van den Bosch, F., Zadoks, J.C., Metz, J.A.J.: Focus expansion in plant disease I. the constant rate of focus expansion. *Phytopathology* **78**, 54-58 (1988)
53. Van den Bosch, F., Zadoks, J.C., Metz, J.A.J.: Focus expansion in plant disease II. realistic parameter-sparse models. *Phytopathology* **78**, 59-64 (1988)
54. Van den Bosch, F., Frinking, H.D., Metz, J.A.J., Zadoks, J.C.: Focus expansion in plant disease III. two experimental examples. *Phytopathology* in press (1988)
55. Van den Bosch, F., Hengeveld, R., Metz, J.A.J., Verkaik, A.J.: A new method for analysing animal range expansion. preprint (1988)
56. Watt, K.E.F.: *Ecology and resource management*. New York: McGraw-Hill 1968
57. Weinberger, H.F.: Asymptotic behaviour of a model in population genetics. In: Chadam, J.M. (ed.) *Nonlinear partial differential equations and applications*. (Lect. Notes in Maths., Vol.648, pp. 47-98) Berlin: Springer 1978
58. Weinberger, H.F.: Long-time behaviour of a class of biological models. *SIAM J. Math. Anal.* **13**, 353-396 (1982)
59. Williamson, E.J.: The distribution of larvae of randomly moving insects. *Australian Journal of Biological Science* **14**, 598-604 (1961)
60. Williamson, M.H., Brown, K.C.: The analysis and modelling of British invasions. *Phil. Trans. R. Soc. London B* **314**, 505-522 (1986)
61. Zadoks, J.C., Kampmeijer, P.: The role of crop populations and their development, illustrated by means of a simulator Epimul 76. *Annals of the New York Academy of Science* **287**, 164-190 (1977)